Annals of Physics **271**, 159–202 (1999)
Article ID aphy.1998.5854, available online at http://www.idealibrary.com on IDEAL®

A High-Precision Study of Anharmonic-Oscillator Spectra

M. H. Macfarlane

Department of Physics and Nuclear Theory Center, Indiana University, Bloomington, Indiana 47405
E-mail: macfarlane@iucf.indiana.edu

Received December 8, 1997

High-precision methods are developed to evaluate eigenvalues for all states $|m, N\rangle$ of the x^{2m} anharmonic oscillators with m from 2 to 6, for all values of the anharmonicity parameter. There are three basic steps: rescaling to introduce a length scale natural to the problem; use of fifth-order JWKB to generate an accurate starting estimate of the rescaled energy; and shifted (resolvent-based) Lanczos algorithm to sharpen the initial JWKB estimate. JWKB itself gives 33-figure accuracy for N greater than 1500 (for $m=2$) to 3500 (for $m=6$). With the JWKB starting energy, the shifted Lanczos algorithm converges to 33 figures in 3 iterations or less for all states. These methods are used in a study of the systematics of anharmonic-oscillator spectra and of the physical effects of the rescaling transformation.

1. INTRODUCTION

This paper describes a fast, economical, and accurate method, based on the JWKB approximation [1] and the shifted or resolvent-based Lanczos algorithm [2–4], for the numerical evaluation of all eigenvalues of the anharmonic-oscillator Hamiltonian

$$H^{(m)} = \tfrac{1}{2}(p^2 + x^2) + \lambda x^{2m} \tag{1}$$

with m from 2 to 6 and $\lambda > 0$. The efficiency of the methods used depends critically on introduction of a natural anharmonic-oscillator length-scale [6, 7]. The resulting rescaled or renormalized eigenvalue problem is finite for all values of the anharmonicity parameter λ. In the infinite-coupling limit it provides the eigenvalues of the pure-oscillator Hamiltonian

$$h^{(m)} = \tfrac{1}{2}p^2 + \lambda x^{2m}. \tag{2}$$

The techniques developed are then used in an extensive study of the systematics of anharmonic-oscillator spectra.

The calculations described here are modest in scale—500 to 1000 kilobytes of memory, running times of a fractions of a second on a PC with a 200-MHz chip. They involve conventional floating-point arithmetic only. All results are accurate to

0003-4916/99 $30.00

working precision—16 significant figures with 64-bit arithmetic, 33 significant figures with 128-bit arithmetic. Extension to higher precision using multi-precision translation packages is straightforward and is discussed at the end of Section 5. Only the 33-figure results will be presented.

Thousands of papers have been written on the quantal anharmonic oscillator [5–11], with no sign yet of waning interest. This reflects the prevalence of Hooke's law and associated vibrational excitations in molecular, condensed-matter and nuclear physics. But there is more to it than that. The anharmonic-oscillator Schrödinger equation is so hard to solve accurately for sizeable values of the coupling parameter λ that it has provided a stringent test of a variety of proposed numerical techniques for the solution of Schrödinger equations [6, 7, 12–15]. Furthermore, the perturbation series for the eigenvalues $E_N^{(m)}$ of the anharmonic-oscillator Hamiltonian (1) has zero radius of convergence; it is an asymptotic expansion, giving limited accuracy for very small values of λ. Since the pioneering work of Bender and Wu [5], the anharmonic-oscillator perturbation series has served as a paradigm for similar asymptotic expansions in many-body physics and field theory. It has played a crucial role in studies of perturbation theory at very high order [16–19] and of ways of summing divergent expansions [20, 21].

The paper is organized as follows. In Section 2, the Hamiltonian of Eq. (1) is subjected to a rescaling transformation (referred to in other studies [6, 7] as renormalization). The essential point is to introduce as length scale for state N of the x^{2m} oscillator that which provides the best variational estimate of its energy. Section 3 discusses methods of calculating the matrix elements of the rescaled Hamiltonian in the rescaled oscillator basis; the issue here is to ensure sufficient accuracy for large quantum numbers to permit 33-figure precision in the final eigenvalues. The JWKB approximation to the energy, carried to fifth order, is studied in Section 4. Its accuracy is found to increase with astonishing rapidity as N increases. For N greater than 1500 (for $m=2$) to 3500 (for $m=6$), fifth-order JWKB gives 33-figure accuracy without further refinement. Even for ground states, errors in the optimal-order JWKB approximation are only a few percent. The JWKB energies developed in Section 4 provide essential input to the shifted Lanczos algorithm, which is discussed in Section 5. The shifted Lanczos algorithm is simply the Lanczos algorithm applied, not to the Hamiltonian H itself, but to its resolvent $(z-H)^{-1}$. If the shift parameter z is close to the desired eigenvalue, the shifted Lanczos algorithm converges rapidly. Using the JWKB energy estimates of Section 4 as shift parameters, 33-figure accuracy is achieved in 3 or fewer Lanczos iterations for all states of interest. Thus the fifth-order JWKB approximation, refined where necessary by the shifted Lanczos algorithm, achieves 33-figure accuracy for the eigenvalues of all states of the x^{2m} oscillators with m from 2 to 6 and all values of the coupling strength λ. Section 6 surveys the systematics of anharmonic-oscillator spectra and discusses the physical effects of the rescaling transformation. The methods used, the range of parameters (m, N, λ) covered and the accuracy achieved in this study are compared in Section 7 with what is to be found in the literature. Section 8 summarizes the main conclusions.

Appendixes A and B give some details pertinent but not central to the discussion in the main text. Appendix A summarizes scaling transformations whereby the eigenvalues of a general anharmonic-oscillator Hamiltonian, in which the potential is an arbitrary linear combination of x^2 and x^{2m} terms, are expressed in terms of those of the reduced Hamiltonian of Eq. (1). The discussion includes the pure-x^{2m} oscillator, which is, in a sense discussed in Section 2, the infinite-coupling limit of the anharmonic oscillator. Finally, different ways of writing the anharmonic-oscillator Hamiltonian appear in the literature. Appendix B gives the necessary formulae to translate energies and other relevant parameters between conventions.

The three linked themes of this study of the anharmonic oscillator are the power of the rescaling transformation, the accuracy of high-order JWKB approximations, and the stability and rapid convergence of the shifted Lanczos algorithm.

2. THE RESCALING TRANSFORMATION

The eigenvalue equation for the anharmonic oscillator is

$$H^{(m)}(\lambda)\,|mN\rangle = E_N^{(m)}\,|mN\rangle. \tag{3}$$

$N=0$ corresponds to the ground state and $N>0$ to the Nth excited state. For $\lambda>0$, the case considered here, the spectrum is discrete, with each eigenvalue $E_N^{(m)}$ growing continuously with λ out of the Nth eigenvalue E_N of the unperturbed harmonic oscillator. States of different parity do not mix. Even-N and odd-N eigenvalue problems are entirely separate.

The eigenvalue problem (3) will be solved in a suitably chosen harmonic-oscillator basis. Use of the basis spanned by the eigenstates of the unperturbed harmonic-oscillator Hamiltonian $\frac{1}{2}(p^2+x^2)$ in Eq. (1) is perfectly feasible. It is, however, much more efficient [6, 7] to use as reference oscillator one whose length-parameter τ^2 is grounded in the physics of the full anharmonic-oscillator problem.

Let the eigenstates of the reference oscillator be given in x-space by

$$\phi_N(x,\tau) = v_N H_N\left(\frac{x}{\sqrt{\tau}}\right)\exp\,-\left(\frac{x^2}{2\tau}\right), \tag{4}$$

where H_N is the Hermite polynomial [22] of degree N and v_N is a normalization constant. There are many possible ways to determine an optimum oscillator length $\sqrt{\tau}$; the simplest and most obvious are the virial and variational conditions. The virial theorem [14, 23, 24] holds for time averages of observables over confined classical motions and for expectation values in quantal bound states. For the anharmonic-oscillator Hamiltonian the virial condition is

$$2\langle T\rangle = \langle p^2\rangle = \left\langle x\frac{dV^{(m)}}{dx}\right\rangle, \tag{5}$$

where $V^{(m)}(x)$ is the potential in Eq. (1). Equation (5) holds for the expectation value in any eigenstate $|mN\rangle$.

Choose as the reference oscillator for state $|mN\rangle$ that for which Eq. (5) holds when the expectation value is taken with the trial wave function (4). The result is a polynomial equation for τ,

$$\lambda G_{mN}\tau^{m+1}+\tau^2-1=0, \tag{6}$$

where

$$G_{mN}=\frac{4m\langle N|\ X^{2m}\ |N\rangle}{(2N+1)}. \tag{7}$$

The rescaled position variable is defined by Eq. (8), below; ways of calculating the matrix element of X^{2m} are discussed in Section 3. The scaling parameter τ is a function of m and N.

Alternatively, the optimal oscillator length may be chosen to minimize the expectation value of the Hamiltonian (1) with respect to the trial wave function (4). The polynomial equation (6) again emerges as variational condition. The fact that, for the anharmonic oscillator, virial and variational conditions coincide stems from the fact that the potential is a polynomial in x.

Only real, positive values of τ are of physical interest; Eq. (6) has one and only one real, positive root for all values of m, N, and $\lambda(\geqslant 0)$. When m is even, Eq. (6) has a single positive root and $m/2$ complex conjugate root-pairs; when m is odd, it has two real roots of opposite sign and $(m-1)/2$ complex conjugate root-pairs. Thus Eq. (6) uniquely specifies an optimal oscillator length. It may be solved to any desired accuracy by a few Newton–Raphson iterations, with any value of τ between 0 and 1 as the starting guess.

Express the Hamiltonian (1) in terms of the rescaled dynamical variables

$$X=x/\sqrt{\tau}, \qquad P=p\sqrt{\tau}, \tag{8}$$

where τ satisfies Eq. (6). The result is [7]

$$H^{(m)}=\frac{\mathscr{H}_N^{(m)}}{\tau} \tag{9}$$

and the rescaled (or renormalized) Hamiltonian is defined by

$$\mathscr{H}_N^{(m)}=\frac{1}{2}(P^2+X^2)+\kappa\left\{\frac{X^{2m}}{G_{mN}}-\frac{1}{2}X^2\right\}. \tag{10}$$

The rescaling transformation preserves the form of the Hamiltonian (1)—an unperturbed harmonic-oscillator Hamiltonian with an anharmonic perturbation; the new effective coupling strength is

$$\kappa = 1 - \tau^2. \tag{11}$$

The perturbing potential in Eq. (10) is the sum of two competing terms—a repulsive X^{2m} term and an attractive X^2 term.

The scale parameter τ is a monotonic decreasing function of λ. This is clear from the fact that the derivative of τ,

$$\frac{d\tau}{d\lambda} = -\frac{G_{mN}\tau^m}{[2 + (m+1)\, G_{mN}\tau^{m-1}]} \tag{12}$$

is negative for finite coupling strengths, approaching zero from below in the infinite-coupling limit. (See Eq. (14).) When λ is small, the first term in Eq. (6) is negligible, so that

$$\tau \to 1 \qquad \text{as} \quad \lambda \to 0. \tag{13}$$

When λ is large, the second term in Eq. (6) is negligible and thus

$$\tau \sim (\lambda G_{mN})^{-1/(m+1)} \sim 0 \qquad \text{as} \quad \lambda \to \infty. \tag{14}$$

In other words, Eq. (6) maps the range $0 \leqslant \lambda < \infty$ on to the finite ranges $[1, 0]$ in τ and $[0, 1]$ in κ. The dependence of τ and κ on λ is illustrated in Fig. 1.

It is now clear why the rescaled Hamiltonian is easier to solve—exactly [7] or perturbatively [21]—than $H^{(m)}$.

(1) The rescaled strength parameter κ cannot exceed 1 in magnitude.

(2) The unbounded growth of the true eigenvalues $E_N^{(m)}(\lambda)$ at large λ has been scaled away (Eq. (15)), leaving a rescaled eigenvalue problem that is finite for all values of the strength-parameter κ.

(3) The effective strength of the term in X^{2m} in the rescaled Hamiltonian is κ/G_{mN}—a small number since G_{mN} is large (of order $(N+\frac{1}{2})^m$) and κ cannot exceed unity. The effects of the reduction in strength of the X^{2m} term will be discussed in Section 6.

The large-λ limit is of particular interest. Let $\mathscr{E}_N^{(m)}(\kappa)$ be an eigenvalue of the rescaled Hamiltonian (10); it follows from Eqs. (9) and (14) that

$$\lim_{\lambda \to \infty} E_N^{(m)} = \gamma_{mN}^0 \lambda^{1/(m+1)}, \tag{15}$$

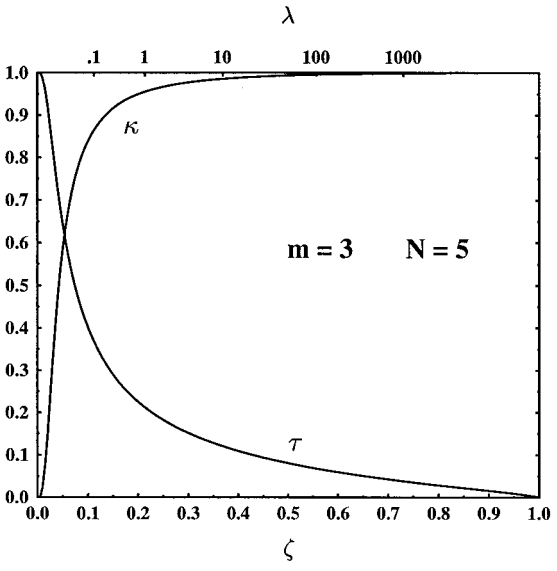

FIG. 1. Scale parameter τ (Eq. (6)) and rescaled coupling parameter κ (Eq. (11)), plotted as a function of the anharmonicity parameter. The abscissa ζ is defined by Eq. (67); equivalent values of λ are shown at the top of the graph.

where

$$\gamma_{mN}^{0} = \mathscr{E}_{N}^{(m)}(1)(G_{mN})^{1/(m+1)} \tag{16}$$

and $\mathscr{E}_{N}^{(m)}(\lambda)$ is the Nth eigenvalue of the rescaled Hamiltonian. Equation (15) is the leading term in the large-λ strong-coupling expansion [9, 16, 25–27]

$$E_{N}^{(m)}(\lambda) = \lambda^{1/(m+1)} \sum_{j=0}^{\infty} \gamma_{mN}^{j} \lambda^{2j/(m+1)} \tag{17}$$

for the anharmonic-oscillator eigenvalues.

As $\lambda \to \infty$, the x^2 term in the Hamiltonian of Eq. (1) becomes negligible relative to the anharmonic term. The large-λ limit of the anharmonic-oscillator eigenvalues, given by Eq. (15), should therefore be the same as that of the eigenvalues of the pure-x^{2m} Hamiltonian of Eq. (2). That this is so follows by setting $\omega = 0$ in the scaling relation (81) derived in Appendix A, which yields

$$h^{(m)}(\lambda) = \lambda^{1/(m+1)} h^{(m)}(1). \tag{18}$$

Thus the eigenvalues of the anharmonic and pure-x^{2m} oscillators are both proportional to $\lambda^{1/(m+1)}$ at large λ. To determine the constant of proportionality, note that

in the infinite-coupling limit ($\kappa = 1$), the rescaled Hamiltonian (10) reduces to pure-x^{2m} form with $\lambda = (G_{mN})^{-1}$. The Nth eigenvalue $\varepsilon_N^{(m)}(\lambda)$ of the pure x^{2m} oscillator is therefore related to the rescaled energy $\mathscr{E}_N^{(m)}(\kappa)$ in the infinite-coupling limit by

$$\varepsilon_N^{(m)}(\lambda) = (\lambda G_{mN})^{1/(m+1)} \mathscr{E}_N^{(m)}(1). \tag{19}$$

This can be expressed more compactly in terms of the infinite-coupling limit constant γ_{mN}^0 defined by Eq. (16),

$$\varepsilon_N^{(m)}(\lambda) = \gamma_{mN}^0 \lambda^{1/(m+1)}, \tag{20}$$

the large-λ asymptotic form of the anharmonic-oscillator energy (Eq. (15)).

To summarize: the infinite-coupling limit constants γ_{mN}^0, the eigenvalues $\varepsilon_N^{(m)}(1)$ of the pure-x^{2m} oscillator at $\lambda = 1$, and the rescaled energies $\mathscr{E}_N^{(m)}(1)$ in the infinite-coupling limit contain exactly the same information. Any of them determine the eigenvalues of the pure-x^{2m} oscillator for all values of λ.

3. CONSTRUCTION OF THE ENERGY MATRIX

This paper deals with the calculation to working precision of all eigenvalues of the x^{2m} anharmonic oscillators with m from 2 to 6. The method used rests on the solution of the rescaled eigenvalue problem

$$\mathscr{H}_N^{(m)}(\kappa)\ |mN\rangle = \mathscr{E}_N^{(m)}(\kappa)\ |mN\rangle \tag{21}$$

in the basis spanned by the eigenfunctions of the rescaled harmonic oscillator Hamiltonian

$$\mathscr{H}_0 = \tfrac{1}{2}(P^2 + X^2) \tag{22}$$

of Eq. (10).

The rescaled eigenvalue problem differs from the original (3) in one important respect—the Hamiltonian $\mathscr{H}_N^{(m)}$ depends explicitly on the state N since both κ and G_{mN} are state-dependent. Two distinct strategies are possible in the search for working-precision eigenvalues for a wide range of states N.

(1) Solve a different eigenvalue problem for each state $|mN\rangle$; in each case only a single eigenvalue—that corresponding to state N—is evaluated.

(2) For each value of m and parity, fix on a single N-independent compromise scale-parameter τ and calculate all desired eigenvalues from this single rescaled Hamiltonian.

The choice here is between evaluation of single eigenvalues of many Hamiltonians and evaluation of many eigenvalues of a single Hamiltonian. The second strategy has two advantages; it yields all eigenvalues in a single basis and

is the approach for which standard numerical techniques for matrix eigenvalue problems have been designed [28]. Its weakness in the anharmonic-oscillator eigenvalue problem lies in the well-documented fact [13] that state-dependent scaling is a crucial ingredient of methods designed to yield accurate eigenvalues for a wide range of states N. The symptom of this weakness is that, when N-independent bases are used, very large dimensions are needed to achieve high precision for many eigenvalues.

This paper adopts the first strategy—evaluation of the single eigenvalue $\mathscr{E}_N^{(m)}$ of the effective Hamiltonian $\mathscr{H}_N^{(m)}$ for each state $|mN\rangle$. The eigenvalue is computed in the basis spanned by the eigenstates $|n\rangle$ of the rescaled harmonic-oscillator Hamiltonian $\mathscr{H}_0$ of Eq. (22). ($\mathscr{H}_0$ and its eigenstates $|n\rangle$ are in fact functions of m, N, and λ, but this dependence is suppressed in the notation to be used.) The orthonormal basis states are defined by

$$\mathscr{H}_0 |n\rangle = (n + \tfrac{1}{2}) |n\rangle, \tag{23}$$

where

$$n = 0, 1, 2, \ldots. \tag{24}$$

The basis states satisfy the orthonormality relations

$$\langle n \mid n' \rangle = \delta_{n, n'}. \tag{25}$$

Only even n enter for even-parity states, odd n for odd-parity states.

The matrix of the rescaled Hamiltonian (10) in this basis is

$$\langle n| \mathscr{H}_N^{(m)} |n'\rangle = \left(n + \frac{1}{2}\right) \delta_{n, n'} + \kappa \left\{ \frac{\langle n| X^{2m} |n'\rangle}{G_{mN}} - \frac{\langle n| X^2 |n'\rangle}{2} \right\}, \tag{26}$$

where the parity of n and n' must be the same. The matrix of X^{2m} ($m \geqslant 1$) is banded

$$\langle n| X^{2m} |n'\rangle = 0 \qquad \text{if} \quad |n - n'| > 2m \tag{27}$$

with half band-width m.[1] Thus the energy matrix for given parity is a real, symmetric band-matrix of half band-width m—a simplifying property of some practical importance for the method of solution developed in Section 5.

Evaluation of energy matrix elements reduces to evaluation of matrix elements of even powers of X between harmonic-oscillator eigenstates. A one-parameter summation formula for matrix elements of all powers of X has been given by Morales and Flores-Riveros [29]. It can be made to give working precision (33 figures in 128-bit arithmetic) for all matrix elements of practical interest for $m = 2$. It loses

[1] m rather than $2m$ because only even or odd states are present.

precision at a rate of about one significant figure for each increase of two units in m. At $m = 6$, it gives at most 30-figure accuracy in 128-bit arithmetic—not enough to give working-precision energy eigenvalues.

An alternative approach is to factor the operator X^{2m} and insert a complete set of intermediate states. With X^2 and $X^{2(m-1)}$ as factors, a recursion formula is obtained for the desired matrix elements;

$$\langle n|\ X^{2m}\ |n'\rangle = \sum_r \langle n|\ X^{2(m-1)}\ |r\rangle\langle r|\ X^2\ |n'\rangle. \tag{28}$$

The matrix of X^2 is of half band-width 1 (for given parity), so that the summation in Eq. (28) runs over at most 3 terms. Since the matrix elements of X^2 can be found in texts on Quantum Mechanics (e.g., [30]), Eq. (28) is a recursion relation giving the matrix-elements of X^{2m} in terms of those of $X^{2(m-1)}$. It can be used numerically or algebraically. Here it is used to derive explicit formulae involving only polynomials in n and square roots of such polynomials for all matrix elements of X^{2m} for m from 2 to 6. The resulting formulae are used in the high-precision eigenvalue calculations reported in this paper. They were derived with the help of the symbolic-algebra program MAPLE [31] and need not be given explicitly here.

Other factorizations of X^{2m} into products of two factors of lower degree yield sum rules similar in form to Eq. (28). They serve as numerical checks on the computed matrix elements.

4. THE JWKB APPROXIMATION

High-order JWKB approximations[2] are known [1] to yield very accurate bound-state energies for particles moving in smooth potential fields. Detailed results have been reported for the quartic anharmonic oscillator [8, 33, 34] and for low eigenvalues of various pure-x^{2m} oscillators [1, 35]. These papers, limited by a lack of sufficiently precise exact eigenvalues for comparison, do not reveal the full accuracy that the JWKB approximation can achieve. This section describes fifth-order JWKB calculations of the rescaled energies of all states of anharmonic oscillators with m from 2 to 6 and all values of the coupling strength. The 33-figure eigenvalues obtained by the shifted Lanczos algorithm described in Section 5 are then used to study the accuracy of the JWKB approximation when carried to fifth non-vanishing order.

High-order JWKB energies of bound states of a particle in a smooth potential can be calculated from a remarkably simple general form of the JWKB quantization

[2] Usually referred to in the physics literature by the letters WKB. This useage slights the contribution of H. Jeffreys whose paper [32] precedes other independent inventions of the method in question by some three years.

condition given by Dunham in a paper [36] published in 1932. The starting point is the standard wave-function transformation

$$\psi(x) = \exp\left[\frac{i}{\hbar}\int^{x} y(t)\,dt\right], \tag{29}$$

which casts the Schrödinger equation for a particle of mass M in a potential $V(x)$ into Riccati–Bessel form

$$\frac{h}{i}\,y'(x) = p^2(x) - y^2(x), \tag{30}$$

where p is the local momentum

$$p(x) = \sqrt{2M(E - V(x))}. \tag{31}$$

The mass M and the constant h have been temporarily restored to exhibit the JWKB approximation as an expansion in powers of h. Substitution of the JWKB expansion

$$y(x) = \sum_{r=0}^{\infty}\left(\frac{h}{i}\right)^{r} y_r(x) \tag{32}$$

in Eq. (30) yields a recursive set of equations for $y_r(x)$ in terms of lower-order coefficient functions and their derivatives. Explicit solutions in terms of the potential V and its derivatives have been given [33, 34] for the functions $y_r(x)$ with r from 0 to 12. For potentials with two classical turning points, Dunham shows that the condition for a bound state at energy E is

$$\oint_C y(z)\,dz = \int_{r=0}^{\infty}\left(\frac{h}{i}\right)^{r}\oint_C y_r(z)\,dz = 2\pi N h, \tag{33}$$

where N is a non-negative integer, $y_r(z)$ is the coefficient in Eq. (32) continued into the complex plane, and C is a closed contour (Fig. 2) encircling the turning points.

Odd y_r with $r > 1$ are exact derivatives of functions that are single-valued on C; their integrals around the closed contour therefore vanish, and they do not contribute to the quantization condition (33). The function $y_1(z)$ is also an exact derivative,

$$y_1(z) = -\frac{1}{4}\frac{d}{dz}\{\ln(E - V)\}, \tag{34}$$

but of a logarithm which is not single-valued on C and gives an integrated contribution of $-\pi h$ to the left-hand side of Eq. (33). Integrals around C of even y_r collapse to integrals along the real axis from the lower turning point (x_1) to the

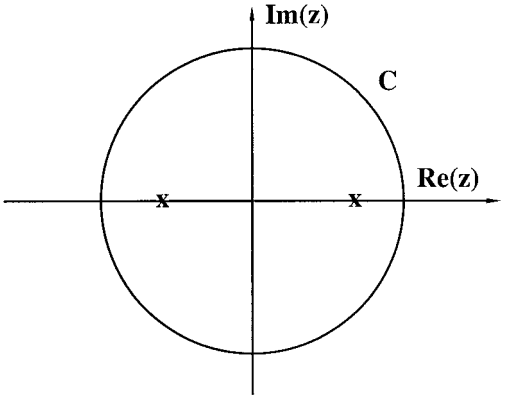

FIG. 2. Contour C for Dunham's form of the WKB quantization condition (Eq. (33)). Crosses indicate the classical turning points.

upper (x_2). The quantization condition, including terms up to $O(h^{2k\,\max})$ on the left-hand side of Eq. (33), is

$$\sum_{k=0}^{k_{\max}} (-)^k I_{2k} = \pi\left(N+\frac{1}{2}\right), \tag{35}$$

where

$$I_{2k} = \int_{x_1}^{x_2} y_{2k}(x)\,dx \tag{36}$$

and units such that $h=1$ and $M=1$ have been restored. The factor $\frac{1}{2}$ on the right-hand side of the quantization condition comes from the $r=1$ term in the JWKB expansion; it is correct only if, as is true in all cases considered here, the derivative of the potential is non-zero at the turning points.

The order of a JWKB approximation will be defined here as the number of terms $(k_{\max}+1)$ included in the series of integrals on the left-hand side of the quantization condition (35). This definition implies that the lowest non-trivial order is the first; leading corrections to ρth order energies are $O(h^{2\rho})$. This paper carries the JWKB approximation to the energies to fifth order; leading corrections are $O(h^{10})$.

For given order, the quantization condition (35) is an implicit equation for the eigenvalues $\mathscr{E}$ (if any) labelled by the integer N. For anharmonic-oscillator Hamiltonians the spectrum is discrete and each eigenvalue is uniquely labelled by a non-negative integer. Solution of the quantization equation for a succession of orders gives a sequence of approximations to the exact energy.

The methods used to construct and solve the JWKB quantization condition are presented here only in outline; details will be given in a separate paper [37].

(1) The JWKB approximation is applied to the rescaled Hamiltonian described in Section 2 rather than to the original Hamiltonian. The point here is

that, as mentioned in Section 2, the rescaling transformation creates a finite eigenvalue problem for all values of the coupling strength. The corresponding JWKB approximations are also finite, which permits high-precision JWKB energies to be evaluated across the full range of coupling strengths.

(2) The JWKB integrals I_{2k} of Eq. (35) are expressed as linear combinations of integrals of the form

$$\int_{-1}^{1} d\xi \frac{\xi^{\alpha}}{\sqrt{1-\xi^2}} (1 + c + \xi^2 + \cdots + \xi^{2(m-1)})^{-v-1/2} \tag{37}$$

for various exponents α and v from -1 to $2(k_{\max} - 1)$. c is defined by

$$c = (2\lambda)^{-1} x_0^{-2(m-1)} \tag{38}$$

with $\pm x_0$ the classical turning points in the anharmonic-oscillator potential. The derivation follows the lines of Refs. [33, 35].

(3) For $m = 2$, the integrals of Eq. (37) can be expressed in terms of complete elliptic integrals of the first and second kinds [33]. For $m \geqslant 3$ the integrals cannot be expressed in terms of standard functions; they are evaluated here, for $m = 2$ as well as for $m \geqslant 3$, by Gauss–Chebyshev quadrature [38, Eq. (4.5.24)]. Up to 250 Gauss points are needed for 33-figure accuracy.

(4) With the integrals I_{2k} calculated in the fashion just outlined, the quantization equation (35) is solved for the energy by Ridder's method [38, Sect. 9.2].

The JWKB expansion Eq. (32) is asymptotic [1]. It is to be expected that the sequence of approximations to the anharmonic-oscillator energy obtained by solving the JWKB quantization condition in successive orders should improve to some optimal accuracy and then deteriorate. The optimum JWKB order—the value of k beyond which the sequence of JWKB approximations to the energy turns around—is found to be almost independent of m and a rapidly increasing function of N. The optimum JWKB order is 2 for $N = 0, 1$; 2 or 3 for $N = 2, 3$; 4 for $N = 4, 5, 6$; 5 or more for $N \geqslant 7$. The rapid increase with N of the optimum order and the accuracy of the JWKB approximation are illustrated in Table I, which shows the relative error

$$\eta = \frac{|\mathscr{E}_{JWKB} - \mathscr{E}|}{|\mathscr{E}|} \tag{39}$$

in the rescaled energy for $m = 6$ and five representative values of N. It is clear from Table I that for large values of N the optimum JWKB order is much greater than 5, and the accuracy attained is far beyond the 33-figure limit of the present study. (This point is made more vividly by Fig. 4, discussed below.)

TABLE I

Relative Error in the kth Order JWKB Approximation to the Energy of State N of the $m=6$ Anharmonic Oscillator, in the Infinite-Coupling Limit.

k	$N=0$	$N=2$	$N=5$	$N=10$	$N=1000$
1	0.46(0)	0.46(−1)	0.88(−2)	0.24(−2)	0.27(−6)
2	0.11(−1)	0.62(−2)	0.13(−3)	0.84(−5)	0.10(−12)
3	0.22(0)	0.39(−2)	0.20(−4)	0.95(−7)	0.17(−18)
4	0.53(0)	0.33(−2)	0.14(−4)	0.31(−7)	0.20(−23)
5	0.64(0)	0.42(−2)	0.17(−4)	0.18(−7)	0.12(−27)

Note. Each entry is to be multiplied by a power of 10 whose exponent is given in parentheses.

The dependence on coupling strength of the accuracy of fifth-order JWKB is illustrated in Fig. 3. There is a region of enhanced accuracy at very small λ because the JWKB approximation has the correct zero-coupling (harmonic oscillator) limit. Beyond this small-λ region (roughly $\lambda > 10^{-5}$) errors are almost independent of the coupling strength. Similar behavior is found for all m and N, although the error curves for small N are sometimes bumpy at small λ because of jumps in the optimum JWKB order.

A complete graphical summary of the accuracy of fifth-order JWKB energies is given in Fig. 4 where the relative error (Eq. (39)) in the infinite-coupling limit is plotted as a function of N for $m=2$ to 6. The accuracy of fifth-order JWKB is seen

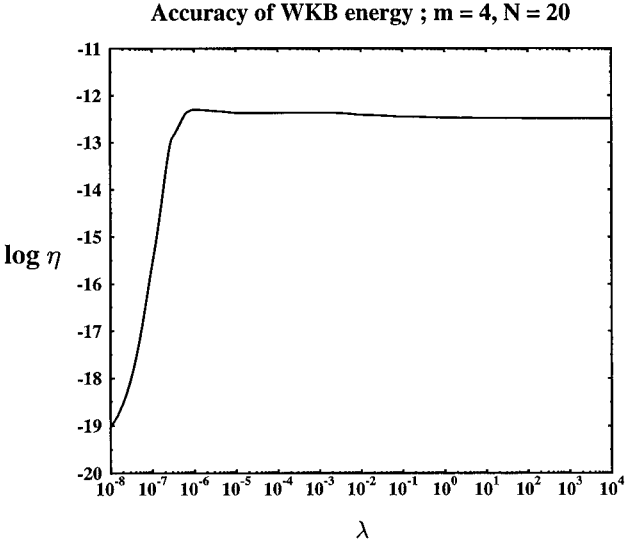

FIG. 3. Relative error (Eq. (39)) in the fifth-order WKB approximation to the rescaled anharmonic-oscillator energy for $m=4$, $N=20$, and λ from 10^{-8} to 10^{4}.

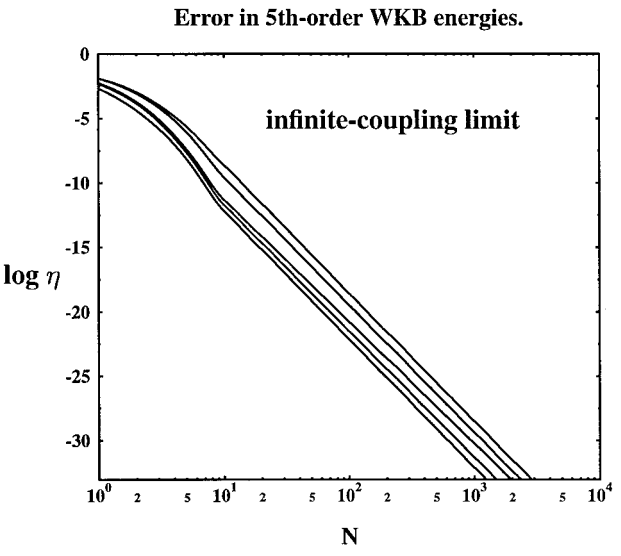

FIG. 4. Relative error (Eq. (39)) in the fifth-order WKB approximation to the rescaled anharmonic-oscillator energy. Errors are shown as a function of N in the infinite-coupling limit for $m=2$ to $m=6$.

to increase very rapidly with increasing N; it surpasses 33 figures at a critical value $N_c(m)$ for which a reasonably close upper bound is given by the linear function

$$N_c = 500(m+1). \tag{40}$$

Even for the lowest states ($N=0$ and $N=1$), the optimal JWKB approximation gives the energies to within 10% or less.

It should be noted that Fig. 4 depicts the accuracy of the JWKB approximation only to fifth order. The full accuracy of the JWKB approximation when carried to optimal order is determined here only for low-lying states. For $N>10$ (or thereabout), the optimal JWKB order is 6 or more—outside the limits of the present study; the relative error clearly drops off faster than linearly with increasing N.

To summarize, the fifth-order JWKB approximation gives anharmonic-oscillator energies with a precision that increases rapidly with N. The accuracy passes 10 figures near $N=10$, 20 figures near $N=150$, and reaches 33 figures at a critical value $N_c(m)$ which ranges from 1500 for $m=2$ to 3500 for $m=6$.

5. THE SHIFTED LANCZOS ALGORITHM

To achieve 33-figure accuracy for anharmonic-oscillator eigenvalues below the critical excitation specified by Eq. (40), the JWKB energy-estimates must be refined. The shifted (resolvent-based) Lanczos algorithm [2] will now be shown to be well

suited to this task of refinement; the fifth-order JWKB energy discussed in Section 2 serves as the shift parameter in the resolvent of the rescaled Hamiltonian.

All variants of the Lanczos algorithm are elaborations of the notion that, for almost any Hermitian matrix A and starting vector $|\phi\rangle$, the sequence $A^k|\phi\rangle$ approaches an eigenvector of A belonging to the numerically largest eigenvalue.

Let A be a non-singular, real, symmetric matrix with a non-degenerate spectrum.[3] The crucial elaboration of the simple iterative scheme mentioned above is the construction of an orthonormal set of vectors $\{|\phi_1\rangle, |\phi_2\rangle, \ldots\}$, referred to as Lanczos vectors. The Lanczos algorithm has the form

$$\begin{aligned} A|\phi_1\rangle &= \alpha_1|\phi_1\rangle + \beta_1|\phi_2\rangle \\ A|\phi_2\rangle &= \beta_1|\phi_1\rangle + \alpha_2|\phi_2\rangle + \beta_2|\phi_3\rangle \\ A|\phi_3\rangle &= \beta_2|\phi_2\rangle + \alpha_3|\phi_3\rangle + \beta_3|\phi_4\rangle \\ &\cdots \end{aligned} \tag{41}$$

Each step introduces a new Lanczos vector $|\phi_k\rangle$. In exact arithmetic, the Lanczos vectors are orthogonal and may be normalized to unity;

$$\langle\phi_k|\phi_{k'}\rangle = \delta_{kk'}. \tag{42}$$

In the orthonormal basis spanned by the first k Lanczos vectors, A is represented by a real, symmetric, tri-diagonal matrix;

$$[A]_k = \begin{bmatrix} \alpha_1 & \beta_1 & & & & & \\ \beta_1 & \alpha_2 & \beta_2 & & & & \\ & \beta_2 & \alpha_3 & \beta_3 & & & \\ & & \ddots & \ddots & \ddots & & \\ & & & \beta_{k-2} & \alpha_{k-1} & \beta_{k-1} & \\ & & & & \beta_{k-1} & \alpha_k & \end{bmatrix}. \tag{43}$$

One of the eigenvalues of $[A]_k$ is an approximation to the numerically largest eigenvalue of A. This approximation has been shown [28] to converge as k increases, provided that the starting vector has not been chosen (perversely) to be orthogonal to the eigensubspace of the desired eigenvalue. As the Lanczos iteration proceeds, other eigenvalues of $[A]_k$ tend toward some of the numerically larger eigenvalues of A.

The Lanczos algorithm in its simplest form (Eq. (41)) has well-known shortcomings in the evaluation of all or many of the eigenvalues of real symmetric matrices [28]. Eigenvalues other than the numerically largest converge slowly. In finite arithmetic, round-off destroys the orthogonality of the Lanczos vectors. Loss

[3] Relaxation of these conditions is of course possible but is irrelevant to the anharmonic-oscillator eigenvalue problem.

of orthogonality has the practical effect of further delaying convergence. If the matrix A is of dimension D, then the Lanczos algorithm with exact arithmetic yields all eigenvalues after D steps. With finite arithmetic, it takes from $2D$ to $5D$ Lanczos steps to exhaust all eigenvalues of large matrices [39]. Many eigenvalues occur repeatedly.

These shortcomings led to the abandonment of the Lanczos algorithm as a general-purpose matrix eigenvalue procedure. In his standard-setting book on the algebraic eigenvalue problem [28], Wilkinson asserts,

> It is difficult to think of any reason why we should use Lanczos' method in preference to Householder's.

In spite of such strictures, the Lanczos algorithm has been widely and successfully used in several areas of many-body quantum physics, particularly in condensed matter [40] and nuclear physics [41]. A reason for favoring the Lanczos algorithm is found in the physics of the many-body problem, where the relevant effective Hamiltonians contain only one-, two-, and occasionally three-body components. This restriction enormously simplifies the task of operating with the Hamiltonian on vectors expressed as linear combinations of individual-particle state-vectors [41]. Efficient application of the Hamiltonian more than compensates for slow convergence to the eigenvalues of interest.

Convergence to eigenvalues in a given region of the spectrum can be accelerated by applying the Lanczos method to the resolvent

$$R(z) = (z - A)^{-1} \tag{44}$$

of the operator or matrix of interest. z is a numerical parameter, in general complex, but restricted in this paper to real values. Matrix and resolvent have common eigenvectors, with eigenvalues related in obvious fashion. The Lanczos iteration converges more rapidly the closer the appropriate eigenvalue of A is to z.

There has been a recent revival of interest in the Lanczos method [2, 3], with extensive applications to the large sparse matrices encountered in structural engineering [4]. The technical development that triggered this new look at the Lanczos procedure is in fact the resolvent strategy outlined above. Its inventors [2] called the modified algorithm "the spectral-transformation Lanczos method," but the alternative name "shifted Lanczos algorithm" seems to have taken root. The parameter z in the resolvent is referred to as the shift parameter. Its choice, or choices if many eigenvalues are sought, is critical to the efficiency of the method.

The potential power of the resolvent strategy was well known to the many-body physicists who used the Lanczos algorithm [41, p. 123]. However, as noted above, many-body applications of the Lanczos method exploit the few-body character of the Hamiltonians used. The associated resolvents are full many-body operators, which fatally impairs the efficiency of the resolvent strategy in many-body applications.

Details will now be presented of the application of the shifted Lanczos algorithm to the central problem of this paper—evaluation to working precision of the Nth eigenvalue of the rescaled anharmonic-oscillator Hamiltonian $\mathscr{H}_N^m$ of Eq. (21). The operator A in Eqs. (41), (43) of the Lanczos algorithm is now to be identified as the resolvent

$$\mathscr{R}_N^{(m)}(z) = (z - \mathscr{H}_N^{(m)})^{-1} \tag{45}$$

of the rescaled Hamiltonian.

Representation of Lanczos Vectors

The Lanczos vectors $|\phi_k\rangle$ are represented by $D_N^{(m)}$-component vectors in the harmonic-oscillator basis of Eqs. (23), (25)

$$|\phi_k\rangle = \sum_{D_N^{(m)}} |n\rangle\langle n \,|\, \phi_k\rangle. \tag{46}$$

The expansion contains $D_N^{(m)}$ basis states of the appropriate parity, distributed as evenly as possible on both sides of the basis state $|N\rangle$ from which the eigenvector $|mN\rangle$ grows. The basis dimension $D_N^{(m)}$ must be chosen large enough that the calculated eigenvalue is unchanged to working precision by extension of the basis. This is discussed later in this section; it is shown that $D_N^{(m)}$ increases slowly with m and, for large N, almost linearly with N. The Lanczos vectors are manipulated as $D_N^{(m)}$-component vectors of real coefficients $\langle n \,|\, \phi_k\rangle$.

Choice of Shift Parameter and Starting Lanczos Vector

Only a single eigenvalue—$\mathscr{E}_N^{(m)}$ of $\mathscr{H}_N^{(m)}$, $(z - \mathscr{E}_N^{(m)})^{-1}$ of $(z - \mathscr{H}_N^{(m)})^{-1}$—is sought for each value of m and N. For each case, z must be chosen as close as possible to the desired energy eigenvalue $\mathscr{E}_N^{(m)}$. The JWKB approximations to the rescaled energies (Section 4) are so accurate that their use as shift parameters results in rapidly convergent Lanczos iterations.

The starting Lanczos vector is chosen as follows. Given the JWKB approximation $\mathscr{E}_{JWKB}$ to the desired eigenvalue of the rescaled Hamiltonian $\mathscr{H}$, the solution $|\phi\rangle$ of the set of inhomogeneous linear equations

$$(\mathscr{H} - \mathscr{E}_{JWKB})\,|\phi\rangle = |\vartheta\rangle, \tag{47}$$

for any vector $|\vartheta\rangle$ is an approximate eigenvector of $\mathscr{H}$ corresponding to eigenvalue $\mathscr{E}_{JWKB}$. This is the first step in the process of inverse iteration [38, Sect. 11.7], a standard method of improving approximate eigenvalues and finding corresponding eigenvectors. A convenient and effective choice for the vector $|\vartheta\rangle$ in Eq. (47) is

$$\langle n \,|\, \vartheta\rangle = \sqrt{\frac{1}{D_N^{(m)}}}, \tag{48}$$

an equally weighted mixture of all basis states. The starting Lanczos vector $|\phi_1\rangle$ is taken to be the solution of the linear equations (47). They are identical in form to those encountered (Eq. (55)) in the implementation of the shifted Lanczos algorithm and are solved in the manner described below.

Implementation of the Shifted Lanczos Algorithm

Formulations of the shifted Lanczos algorithm that are equivalent in exact arithmetic may suffer quite different round-off errors in finite arithmetic. Paige [42] has compared the various possibilities and identified one that minimizes round-off error; it has been used in all subsequent applications and is used here.

The kth step of the Lanczos iteration (42), with the matrix A replaced by the resolvent $\mathscr{R}$ of Eq. (45), is then as follows. The previous $k-1$ steps have determined the sequence $\{|\phi_1\rangle, |\phi_2\rangle, ..., |\phi_k\rangle\}$ of Lanczos vectors, and also the diagonal elements $(\alpha_1, \alpha_2, ..., \alpha_{k-1})$ and the off diagonal elements $(\beta_1, \beta_2, ..., \beta_{k-1})$ of the Lanczos matrix. Then

$$|v_k\rangle = \mathscr{R}_N^{(m)} |\phi_k\rangle - \beta_{k-1} |\phi_{k-1}\rangle, \tag{49}$$

$$\alpha_k = \langle \phi_k | v_k \rangle, \tag{50}$$

$$|w_k\rangle = |v_k\rangle - \alpha_k |\phi_k\rangle, \tag{51}$$

$$\beta_k = \sqrt{\langle w_k | w_k \rangle}, \tag{52}$$

$$|\phi_{k+1}\rangle = \frac{|w_k\rangle}{\beta_k}. \tag{53}$$

The Lanczos process begins with only the starting vector specified and ends when the appropriate eigenvector of the Lanczos matrix (43) has converged to desired accuracy.

Action of Resolvent on Lanczos Vectors

Each Lanczos iteration starts with the operation

$$|\chi_k\rangle = \mathscr{R}_N^{(m)} |\phi_k\rangle = (z - \mathscr{H}_N^{(m)})^{-1} |\phi_k\rangle \tag{54}$$

of an inverse operator on a known vector. This operation is implemented by solution of the inhomogeneous linear equations

$$(z - \mathscr{H}_N^{(m)}) |\chi_k\rangle = |\phi_k\rangle. \tag{55}$$

Now $(z - \mathscr{H}_N^{(m)})$, like $\mathscr{H}_N^{(m)}$, is a symmetric band matrix of half band-width m. Its LU decomposition [38, Sect. 2.3] into a product of lower- and upper-triangular factors

$$z - \mathscr{H}_N^{(m)} = LU \tag{56}$$

preserves band-structure [43, Sect. 2.2]. L and U are band matrices with half bandwidth $m+1$. The LU decomposition is carried out by standard methods [43, Sect. 2.2] before the start of the series of Lanczos iterations and need not be repeated. (The fact that the matrix $(z-\mathscr{H}_N^{(m)})$ is not positive definite precludes use of the simpler Cholesky decomposition [38, Sect. 2.9] in which LU reduces to LL^T.)

Given the triangular factors L and U, the linear equations (55) are solved in two stages, with an intermediate vector $|y\rangle$:

$$L|y\rangle = |\phi_k\rangle, \tag{57}$$

$$U|\chi_k\rangle = |y\rangle. \tag{58}$$

Solution of each set of equations is a simple sequence of substitutions, from the upper tip of the triangle down in Eqs. (57), from the lower tip up in Eqs. (58).

The fact that the LU decomposition preserves band structure adds greatly to the efficiency of the shifted Lanczos algorithm in the anharmonic-oscillator eigenvalue problem.

Eigenvalue Determination; *Convergence Criterion*

The kth Lanczos matrix $[\mathscr{R}_N^{(m)}]_k$ (cf. Eq. (43)) is available after completion of the kth Lanczos iteration. It remains to extract the eigenvalue $[\rho_N^{(m)}]_k$ such that

$$[\mathscr{E}_N^{(m)}]_k = z + [\rho_N^{(m)}]_k^{-1} \tag{59}$$

best approximates the single desired eigenvalue $\mathscr{E}_N^{(m)}$ of the rescaled Hamiltonian $\mathscr{H}_N^{(m)}$. The procedure used here is as follows. All k eigenvalues of $[\mathscr{R}_N^{(m)}]_k$ are evaluated; this is a minor computational task since the Lanczos iterations converge with such extraordinary rapidity that k never exceeds 3. That eigenvalue is selected for which the kth approximation to $\mathscr{E}_N^{(m)}$, calculated from Eq. (59), is closest to the $(k-1)$st approximation. The selected resolvent-eigenvalue is invariably by far the largest.

The Lanczos iteration terminates when the desired eigenvalue has been fixed to a relative error less than some pre-assigned accuracy-parameter ε;

$$\left| \frac{[\mathscr{E}_N^{(m)}]_k - [\mathscr{E}_N^{(m)}]_{k-1}}{[\mathscr{E}_N^{(m)}]_k} \right| \leqslant \varepsilon. \tag{60}$$

For 33-figure accuracy in the energy-eigenvalues, it suffices to set the accuracy parameter at

$$\varepsilon \simeq 2 \times 10^{-34}. \tag{61}$$

Basis Dimensions

The minimum basis dimension $D_N^{(m)}$ for 33-figure accuracy is determined empirically by extending the basis (in the symmetric fashion discussed following Eq. (46))

until the eigenvalue $\mathscr{E}_N^{(m)}$ stabilizes. The minimum dimension increases with m—a feature common to most methods of solution of the anharmonic-oscillator eigenvalue problem. Its dependence on λ is so slight that it may be ignored. For fixed m, $D_N^{(m)}$ varies little with N up to about $N=200$; thereafter a steady increase sets in that is almost linear for $N>1000$. The dependence of $D_N^{(m)}$ on m and N is adequately parameterized by the relation

$$D_N^{(m)} = A_m + B_m N \tanh \omega_m N, \tag{62}$$

where it is understood that the integer part of the expression is to be taken. A_m is the basis dimension needed for $N=0$, $A_m + B_m$ for $N \to \infty$. Values of the parameters are given in Table II. This estimate of the minimum basis dimension is conservative in the sense that it gives a basis large enough for 33-figure accuracy for $2 \leqslant m \leqslant 6$, all N and all κ, usually with something to spare.

The size of the oscillator basis needed for given accuracy is independent of the method used to extract eigenvalues. The minimum basis dimensions summarized by Eq. (62) and Table II have also been derived (with much greater computational labor) using the Jacobi method [38, Sect. 11.1] to diagonalize the rescaled energy matrix.

That large oscillator bases are needed is readily understood. The eigenfunctions of the x^{2m} anharmonic oscillator fall off at large $|x|$ as

$$\exp\left[-\frac{|x|^{m+1}}{(m+1)} \right]. \tag{63}$$

A harmonic-oscillator expansion seeks to simulate this behavior by a linear combination of products of polynomials and Gaussians.

The unbounded increase of $D_N^{(m)}$ with N eventually defeats any method of solution of the anharmonic-oscillator eigenvalue problem in a harmonic-oscillator basis. This trap is avoided in the present study because the accuracy of the JWKB approximation for large N makes explicit matrix diagonalization unnecessary for $N>500(m+1)$. The largest basis dimension encountered is about 1500.

TABLE II

Coefficients in the Expression Given in the Text for the Minimum Basis Dimension

m	A_m	B_m	ω_m
2	102	0.278	0.0045
3	150	0.329	0.0030
4	257	0.349	0.0008
5	527	0.340	0.00035
6	700	0.330	0.00026

Convergence of the Lanczos Iterations

The shifted Lanczos procedure, with JWKB shift parameter, will now be shown to converge very rapidly for all values of m, N, and all values of the coupling strength.

For the lowest states ($N \leqslant 10$), where the JWKB approximation to the rescaled energy is least accurate, the rate of convergence can be improved, and its dependence on m and N all but eliminated, by adoption of a two-stage strategy, restarted with an improved shift parameter.

(1) Carry out k_1 Lanczos iterations with the usual starting vector and shift parameter. An estimate $[\mathscr{E}_N^{(m)}]_{k_1}$ of the rescaled energy is obtained.

(2) Use this estimate as an improved shift parameter. Restart and carry out k_2 Lanczos iterations.

Restarting the Lanczos algorithm might be thought to incur a significant numerical penalty, since the LU decomposition (Eq. (56)) of the resolvent must be reconstructed. It is found that k steps of the restarted algorithm involve about the same effort as $k + \frac{1}{2}$ uninterrupted Lanczos iterations. Since restarting saves one iteration, there is a small net gain in computational efficiency.

Numerical experiments reveal that the restarted Lanczos procedure with

$$k_1 = 2, \qquad k_2 = 1 \tag{64}$$

yields 33-figure accuracy for all m, N, and κ. This is illustrated in Table III for $m = 6$ and four representative values of N, in the infinite-coupling limit.

For $m = 6$, three restarted Lanczos iterations are needed for $N = 0$, two iterations for $N = 10$ and $N = 20$, and only one iteration for $N = 30$. This pattern of a rapid decrease with N of the number of Lanczos iterations needed to give 33-figure accuracy in the energies is repeated for all values of m and all values of the coupling strength. The values of N at which the transitions from 3 iterations to 2 and from 2 to 1 occur are linear functions of m as shown in Fig. 5;

$$N_t(m; 3 \to 2) = m + 2 \tag{65}$$

$$N_t(m; 2 \to 1) = 4m. \tag{66}$$

Since JWKB alone gives 33-figure accuracy for $N \geqslant 500(m+1)$, no more than 3 Lanczos iterations are needed to give working-precision rescaled energies for all states of the anharmonic oscillators with $2 \leqslant m \leqslant 6$.

Orthogonality of the Lanczos Vectors

Round-off error is expected to destroy the orthogonality of the Lanczos vectors $|\phi_k\rangle$ after many iterations. It was shown by Paige [44] that significant loss of orthogonality arises immediately after an eigenvalue has converged and involves errors in the components of the Lanczos vectors in the direction of the converged eigenvector. Since the Lanczos calculations in this paper seek only one eigenvalue

TABLE III

Convergence of Lanczos Iterates $\mathscr{E}_k$ to the Rescaled Energy of Four States of the $m = 6$ Anharmonic Oscillator, in the Infinite-Coupling Limit

k	$\mathscr{E}_k$
	$N = 0$
	0.22585919122322857264956637606437 8
1	0.23106456200722379904107216437035 8
2	0.23106454736849493316210451771241 0
3	0.23106454736849061242868144037282 6
4	0.23106454736849061242868144037282 6
	$N = 10$
	6.44970704360979177293563009649081
1	6.44970692836631711304511294373711
2	6.44970692836631711304679695293149
3	6.44970692836631711304679695293149
	$N = 20$
	12.72734873582173378766023735872 40
1	12.72734873569367096707814570646 03
2	12.72734873569367096707814570646 22
3	12.72734873569367096707814570646 22
	$N = 30$
	18.97698650404072116965358016418 78
1	18.97698650403735522427569940329 87
2	18.97698650403735522427569940329 87

Note. The top line in each section is the initial JWKB estimate.

from each matrix and involve at most 3 Lanczos iterations, significant loss of orthogonality seems unlikely. This expectation is confirmed in practice. The Lanczos vectors for the rescaled anharmonic oscillator, computed according to Eqs. (49) to (53), are orthonormal to working precision; explicit re-orthogonalization changes neither intermediate nor final results of the Lanczos iteration.

Verification of Correctness

Convergence to 33 figures does not necessarily imply correctness to the same degree of accuracy. Three distinct checks confirm the correctness of the anharmonic-oscillator energies calculated in this paper.

The first category of check is internal and addresses the issue of 33-figure correctness directly. Eigenvalues calculated by the shifted Lanczos algorithm are compared

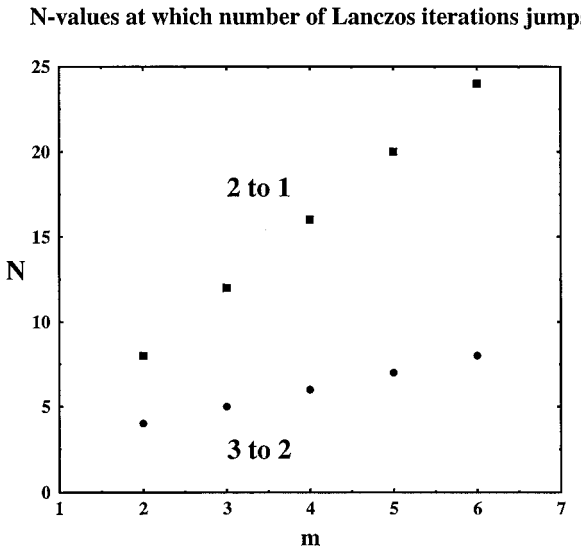

FIG. 5. Transition values $N_t(m)$ (Eqs. (65) and (66)) of the state parameter N at which the number of Lanczos iterations needed to give energies correct to 33 figures changes from 3 to 2 (circles) and from 2 to 1 (squares).

with those obtained by direct diagonalization of the rescaled Hamiltonian matrix (Eq. (26)). The direct diagonalization is carried out by the inefficient but foolproof Jacobi method [38, Sect. 11.1]. Hundreds of spot-checks[4] over a wide range of parameters yield agreement to 33 figures.

A possible source of error is convergence, not to the desired eigenvalue of the rescaled Hamiltonian, but to a spurious neighbor. This possibility can be eliminated decisively. The JWKB approximation is accurate to less, usually much less, than the nearest-neighbor level-spacing. Thus the close agreement obtained between calculated eigenvalues and their JWKB approximants verifies convergence to the correct eigenvalue.

Finally, the eigenvalues obtained by the shifted Lanczos algorithm have been checked extensively against published results. Most of these results concern the quartic oscillator ($m = 2$), nothing is available for $m > 5$ and the accuracy of most previous studies is much less than 33 figures. Within their limitations, published results confirm the correctness of the shifted-Lanczos eigenvalues. These comparisons are discussed in more detail in Section 7.

Multi-Precision Extension

The methods described above have no intrinsic limitation to 33-figure accuracy. A multi-precision translation package developed by Bailey [45] permits the

[4] This comparison does not address the accuracy of the calculated energy matrix elements. That these matrix elements are correct to 33 figures is established by the sum-rule checks described in Section 3.

Fortran programs used in this study to be converted to much higher precision. Convergence up to 80 figures has been achieved for a random selection of anharmonic-oscillator eigenvalues. The size of the oscillator basis, the number of Lanczos iterations, and the running times increase steadily with the precision demanded.

Summary

The shifted Lanczos algorithm, with the JWKB energy as shift parameter, permits calculation of anharmonic-oscillator eigenvalues to 33 figures in at most 3 iterations. For $N \geqslant 24$, 1 iteration is sufficient. For $N > N_c$, where N_c is the critical value of N given by Eq. (40), JWKB itself gives 33-figure accuracy and Lanczos refinement is unnecessary.

6. ANHARMONIC-OSCILLATOR SPECTRA

This section analyzes the systematics of anharmonic-oscillator spectra. The discussion covers the dependence of the true and rescaled energies on the parameters m, N, and λ, the pure-x^{2m} oscillator limit, and the remarkable simplification brought about by the rescaling transformation. True energies are shown in Figs. 6 to 12, rescaled energies (in units of τ) in Figs. 13 to 17.

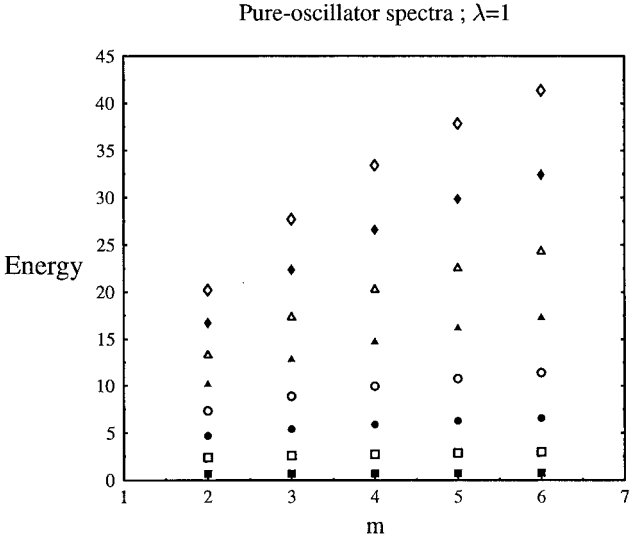

FIG. 6. Lowest eigenvalues of the pure-oscillator Hamiltonians (Eq. (2)) with $m = 2$ to $m = 6$ and $\lambda = 1$. The states included are $N = 0$ (filled squares), $N = 1$ (open squares), $N = 2$ (filled circles), $N = 3$ (open circles), $N = 4$ (filled triangles), $N = 5$ (open triangles), $N = 6$ (filled diamonds), and $N = 7$ (open diamonds).

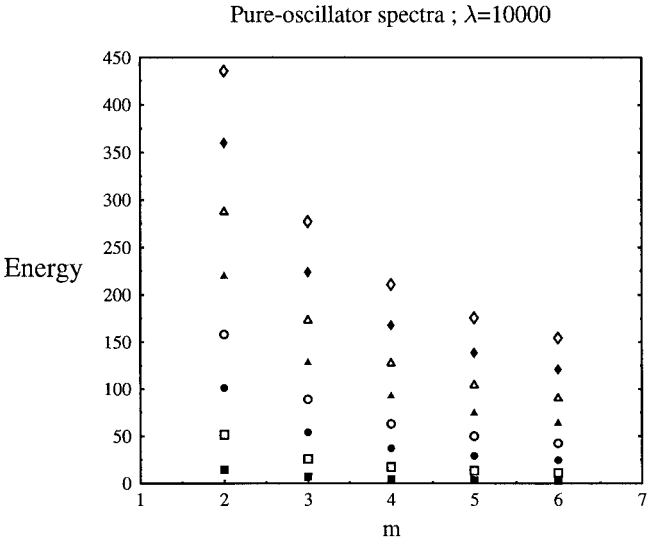

FIG. 7. Lowest eigenvalues of the pure-oscillator Hamiltonians (Eq. (2)) with $m=2$ to $m=6$ and $\lambda=10^4$. For interpretation of the symbols, see the caption to Fig. 6.

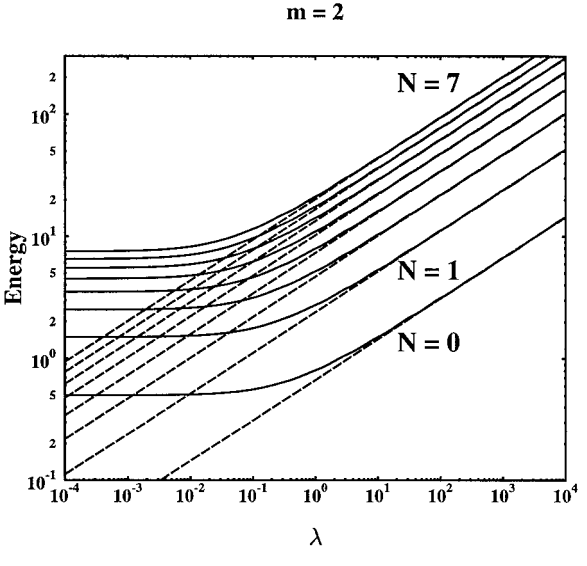

FIG. 8. The eight lowest energy-eigenvalues of the anharmonic and pure-x^{2m} oscillators with $m=2$ as functions of the anharmonicity parameter λ. The dashed lines represent the pure-oscillator energies.

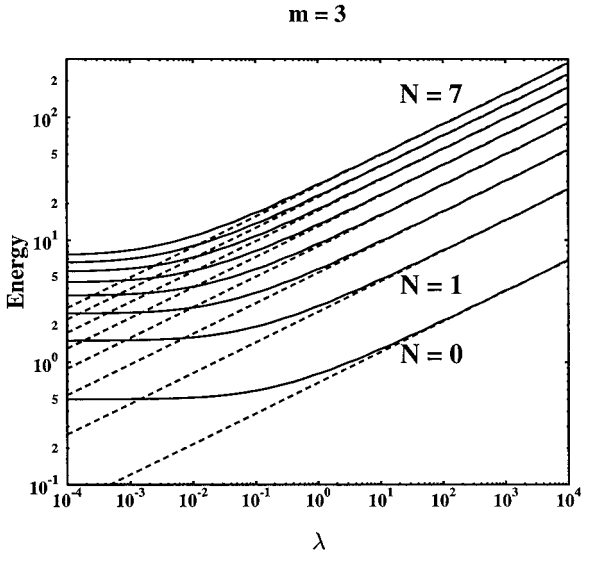

FIG. 9. The eight lowest energy-eigenvalues of the anharmonic and pure-x^{2m} oscillators with $m = 3$ as functions of the anharmonicity parameter λ. The dashed lines represent the pure-oscillator energies.

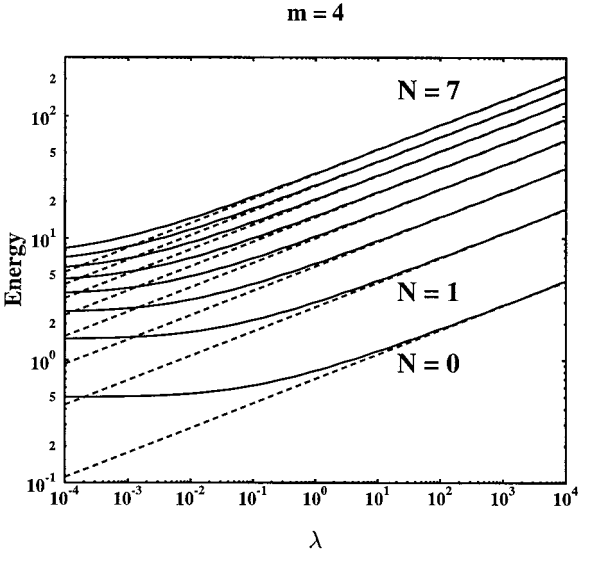

FIG. 10. The eight lowest energy-eigenvalues of the anharmonic and pure-x^{2m} oscillators with $m = 4$ as functions of the anharmonicity parameter λ. The dashed lines represent the pure-oscillator energies.

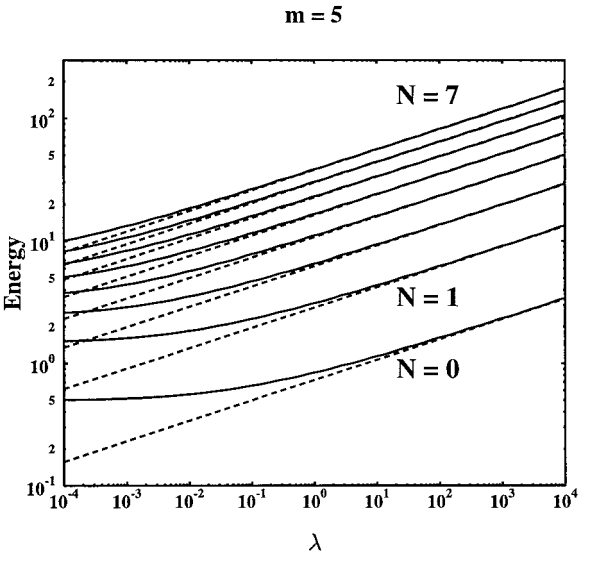

FIG. 11. The eight lowest energy-eigenvalues of the anharmonic and pure-x^{2m} oscillators with $m=5$ as functions of the anharmonicity parameter λ. The dashed lines represent the pure-oscillator energies.

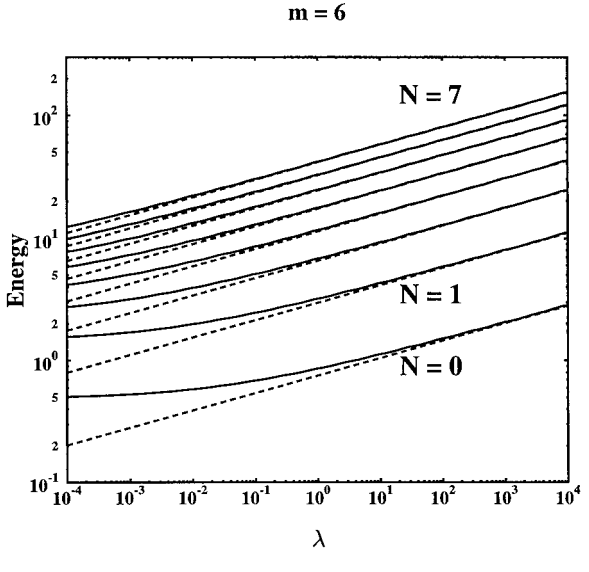

FIG. 12. The eight lowest energy-eigenvalues of the anharmonic and pure-x^{2m} oscillators with $m=6$ as functions of the anharmonicity parameter λ. The dashed lines represent the pure-oscillator energies.

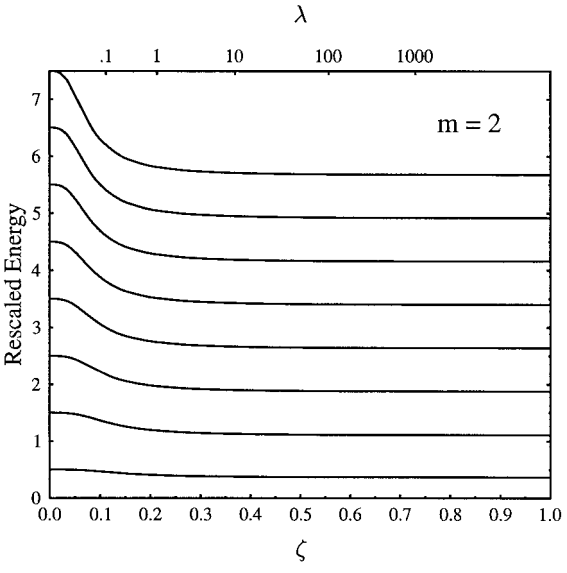

FIG. 13. Rescaled energies of the eight lowest states of the $m = 2$ anharmonic oscillator as functions of the anharmonicity parameter ζ. τ and ζ are defined by Eqs. (6) and (67).

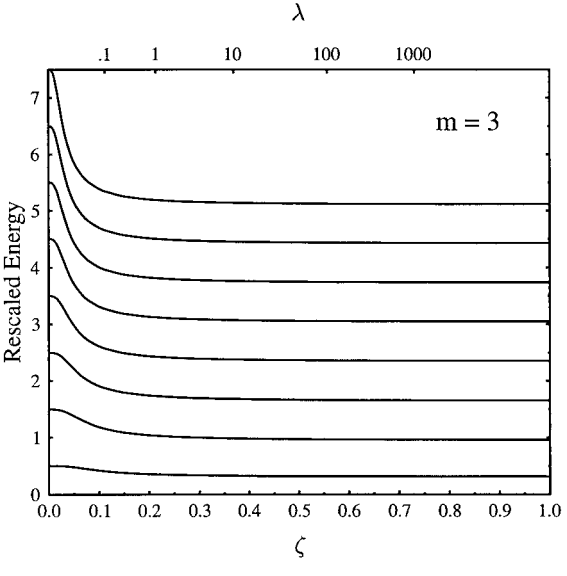

FIG. 14. Rescaled energies of the eight lowest states of the $m = 3$ anharmonic oscillator as functions of the anharmonicity parameter ζ. τ and ζ are defined by Eqs. (6) and (67).

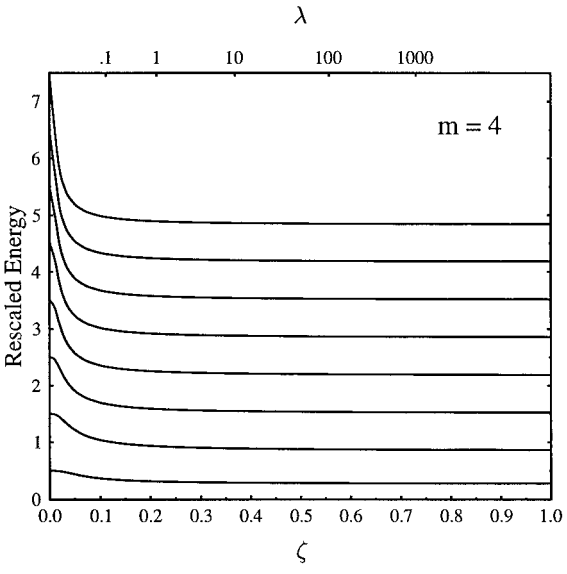

FIG. 15. Rescaled energies of the eight lowest states of the $m = 4$ anharmonic oscillator as functions of the anharmonicity parameter ζ. τ and ζ are defined by Eqs. (6) and (67).

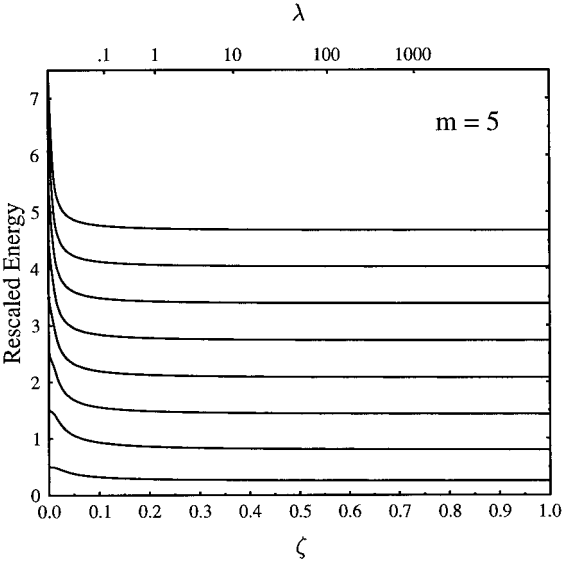

FIG. 16. Rescaled energies of the eight lowest states of the $m = 5$ anharmonic oscillator as functions of the anharmonicity parameter ζ. τ and ζ are defined by Eqs. (6) and (67).

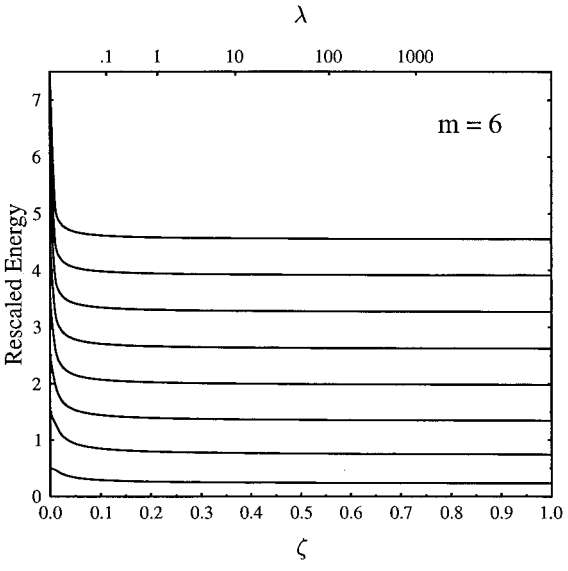

FIG. 17. Rescaled energies of the eight lowest states of the $m=6$ anharmonic oscillator as functions of the anharmonicity parameter ζ. τ and ζ are defined by Eqs. (6) and (67).

The 8 lowest energy eigenvalues ($N=0\cdots7$) of the pure-x^{2m} oscillators with m from 2 to 6 are shown for $\lambda=1$ in Fig. 6, for $\lambda=10^4$ in Fig. 7. The diagrams show that for a given state N the pure-oscillator energy $\varepsilon_N^{(m)}$ increases monotonically with m for small λ, decreases monotonically for large λ. This switch in m-dependence between small and large values of λ, also evident in the JWKB energies, is discussed (for m from 2 to 4) in Ref. [46]. Pure-oscillator energies are also shown in Figs. 8 to 12 where the emphasis is on their relation to anharmonic-oscillator energies.

The anharmonic-oscillator energies $E_N^{(m)}(\lambda)$ and the corresponding pure-x^{2m} oscillator energies $\varepsilon_N^{(m)}(\lambda)$ are shown in Figs. 8 to 12 for the 8 lowest states ($N=0\cdots7$), with m from 2 to 6, over the range ($10^{-4}\leqslant\lambda\leqslant10^4$) of the strength parameter. Both axes in these diagrams are logarithmic. The $\lambda^{1/(m+1)}$ dependence of the pure-oscillator energies is represented by dashed straight lines of slope $1/(m+1)$. The anharmonic-oscillator energies heal to these straight lines at large λ.

Figure 8 for the quartic oscillator ($m=2$) reproduces Fig. 1 of Hioe *et al.* [25], who identify three regions in the (N,λ)-plane:

(1) the near-harmonic-region at small λ,

(2) the pure-x^{2m} region at large λ,

(3) a connecting or boundary layer between the small- and large-λ regions.

Hioe *et al.* propose different methods of solution and different approximation techniques for the anharmonic-oscillator Schrödinger equation in different regions. This subdivision of the (N,λ)-plane is evident for all values of m from 2 to 6 in

Figs. 8 to 12. The near-harmonic region is the set of horizontal plateaux to the left of the energy-curves. The pure-x^{2m} region is defined by the asymptotic large-λ straight lines of slope $1/(m+1)$. The boundary layer consists of the short connecting arcs.

Suppose that the values of λ at which one region merges with another are defined in some reasonable but unspecified fashion. It is clear from Figs. 8 to 12 that the connecting points move toward smaller λ as N increases for given m and toward larger λ as m increases for given N. The length of the boundary region decreases with increasing N, increases with increasing m.

The rescaled energies present a different and simpler view of the energy systematics. It is possible and desirable to exhibit the rescaled energies over the full range of coupling strengths, from zero to the infinite-coupling limit. This requires a suitable mapping of the infinite range $0 \leqslant \lambda < \infty$ on to a finite interval. The scale parameter τ and the rescaled coupling parameter κ introduced in Section 2 define mappings on to the interval $[0, 1]$. They are, however, unsuitable for graphs showing the energies of many states N for given m because they are explicitly state-dependent. Furthermore, as illustrated in Fig. 1, the τ- and κ-mappings compress most of the λ-range into miniscule regions near the infinite-coupling limit. A suitable plotting variable, arrived at by trial and error and devoid of theoretical significance, is defined by

$$\zeta = \frac{\lambda^{1/3}}{\lambda_0^{1/3} + \lambda^{1/3}} \tag{67}$$

with $\lambda_0 = 50$, which maps the full λ-range on to $0 \leqslant \zeta \leqslant 1$.

The rescaled energies $\mathscr{E}_N^{(m)}(\lambda)$ of the 8 lowest states ($N = 0 \cdots 7$) with $m = 2$ to 6 are shown as functions of the strength parameter ζ in Figs. 13 to 17. Values of the original strength parameter λ appear at the top of each diagram. State labels are omitted: they can be read from the $\zeta = 0$ limits of the energy curves ($(N + 1/2)$ for all values of m).

The rescaled energy-curves are simpler than the true-energy curves and of different character. Each curve drops from the harmonic limit to a level plateau that sets in at very small values of λ ($\leqslant 0.1$) and extends with little change in energy to the infinite-coupling limit ($\zeta = 1$). Recall now that the rescaled coupling parameter κ (Fig. 1) maps almost the entire λ-range into a tiny region close to the infinite-coupling limit ($\kappa = 1$). This has an important consequence for the rescaled energies; values of κ deviate very little from 1 over the entire plateau regions. The rescaled eigenvalue problem at any point in a plateau, that is, for any value of λ greater than about 0.1, is essentially the same as in the infinite-coupling limit. Any point below the plateau is clearly in the near-harmonic regime. In other words, the rescaling transformation collapses the three regions of the true energy curves into two—the near-harmonic region of very small λ and the nearly pure x^{2m} region everywhere else.

The change in shape between the true and rescaled energy-curves can be related to the λ-dependence of the scale parameter $\tau(\lambda)$, by which the true energy must be

multiplied (Eq. (9) and Fig. 1) to obtain the rescaled energy. In the small-λ region in which the rescaled energy falls rapidly, the true energy varies slowly, while τ decreases rapidly from 1 to very small values. Thus the small-λ decrease of the rescaled energies simply mirrors the small-λ behavior of τ. It has already been remarked that the large-λ behavior of $1/\tau$ ($\propto \lambda^{1/(m+1)}$) is identical to that of the true energies. This accounts for the large-λ plateaux of the rescaled energy curves; the early onset of these plateaux implies that the parameter τ has the same λ-dependence as the true energies not only in the asymptotic regime but throughout the boundary layer as well.

The rescaled energies are less than the harmonic limit for all non-zero values of λ. This implies that the net effect of the effective potential

$$V_N^{(m)} = K\left\{\frac{X^{2m}}{G_{mN}} - \frac{1}{2}X^2\right\} \tag{68}$$

in the rescaled Hamiltonian (10) is attractive. The factor $(G_{mN})^{-1}$ is so small that the repulsive anharmonic term always loses the competition with the attractive X^2 term.

The results of this section reveal the main qualitative effect of rescaling. It is to replace the anharmonic-oscillator eigenvalue problem by a rescaled transform that is not only finite for all values of the strength parameter λ but almost independent of λ. The rescaled energies and the internal details of their calculation are almost the same for $\lambda = 0.1$ as they are in the infinite-coupling limit. The pure-x^{2m} oscillator is now to be regarded as a rather uninteresting special case of the anharmonic oscillator. The view that has been usual in the literature treats the pure-x^{2m} oscillator as something distinct from its anharmonic cousin. Rescaling makes such a distinction senseless.

7. COMPARISON WITH OTHER STUDIES

How do the methods and results presented here compare with what is available in the literature? This question is addressed in a survey of papers which evaluate anharmonic-oscillator energy eigenvalues or high-precision approximations thereto. The survey is of necessity incomplete. Its limited aim is to cite and discuss the main competing techniques and the most extensive compilations of numerical results.

Papers are classified by method. With one exception, the published eigenvalues are less accurate, usually much less accurate, than those reported here. All eigenvalues in the papers cited have been compared with the JWKB–Lanczos results that are the main topic of this paper. In almost all cases, there is agreement[5] to a single unit in the last figure of the less-accurate result. Exceptions will be noted explicitly.

[5] With due attention to differences in the normalization of the Hamiltonian (see Appendix B).

The various different methods used are less different than first meets the eye. Most involve expansion in an unperturbed harmonic-oscillator basis, rescaled or not. The major exception—apart from series approximations such as JWKB and perturbation theory—is the recursive moment approach of Richardson and Blankenbecler [15].

Method of Hill Determinants

The majority of papers on anharmonic-oscillator eigenvalues use the Hill-determinant method, usually attributed to Bazley and Fox [47]. The basic idea is to expand the wave function $\psi_N^{(m)}(x)$ in the anharmonic-oscillator Schrödinger equation (3) in a series of the form

$$\psi(x) = \exp(-\tfrac{1}{2}x^2) \sum_{n=0}^{\infty} c_n x^{\varepsilon+2n}, \tag{69}$$

where ε is 0 for even states, 1 for odd states. This is equivalent to an expansion in harmonic-oscillator eigenstates with a fixed length scale. Substitution in the Schrödinger equation yields an $(m+1)$-term recursion equation for the expansion coefficients. The recursion relation has non-trivial solutions at the zeros of a banded determinantal function of the energy. The Hill-determinant method in its simplest form demands finding the zeros of this non-linear determinantal function.

Biswas *et al.* [12] use the Hill-determinant method in the earliest extensive study of anharmonic-oscillator spectra. They give eigenvalues for $m=2$ ($N=2$ to 8), $m=3$ and $m=4$ ($N=0$ and $N=1$), each for λ from 0.1 to 100. The $m=2$ ground-state eigenvalue is given to 15 figures, other $m=2$ energies to 8 figures, $m=3$ energies to 7 figures, and $m=4$ energies to 3 or 4 figures.

The steady decrease of accuracy with m evident in the results of Biswas *et al.* stems from the inability to keep up with the rapid growth in the size of basis needed in the expansion (69). This increase is much more rapid than that encountered in Section 5 since rescaling greatly limits the size of basis needed for given precision. Banerjee *et al.* [13, 46] note that a state-dependent length-scale in the trial wave function (69) reduces the size of basis needed and hence permits greater accuracy for a given amount of computational labor. They replace the fixed Gaussian in Eq. (69) by

$$\exp[-\tfrac{1}{2}\alpha_N^{(m)} x^2] \tag{70}$$

and adjust the state-dependent scale factor α empirically to reduce basis dimensions. This first step toward full rescaling permits Banerjee *et al.* to achieve 15-figure accuracy for a sizeable range of oscillator parameters: m from 2 to 4, N from 0 to 10^4, λ in ten steps from 10^{-5} to 4×10^4, and the pure-x^{2m} oscillator with $\lambda=1$.

The Hill-determinant method would gain in efficiency both by application to the rescaled Hamiltonian and by use of the excellent starting guess provided by the JWKB approximation. It is possible that such embellishments would forge a

method comparable in efficiency to JWKB–Lanczos; in the absence of careful numerical studies, this must remain a speculation.

Extensions of the Hill-Determinant Method

The large number of states needed in the expansion (69) or its rescaled variant stems from the attempt to represent wave functions with an asymptotic decrease much faster than Gaussian (Eq. (63)) as linear superpositions of Gaussians. This suggests generalization of the exponential factor (70) to something like

$$\exp[-(\alpha x^2 + \beta x^4)], \tag{71}$$

with both parameters α and β state-dependent. Inclusion in the Hill-determinant trial function of mixtures of different exponentials was first proposed by Datta and Mukherjee [48]. Criticisms soon followed. It was suggested [49–51] that the generalized Hill determinants have zeros that do not correspond to anharmonic-oscillator energy eigenvalues; doubt was thus cast on the results of Banerjee *et al.* and of earlier studies based on the Hill-determinant method.

The current state of understanding is as follows:

(1) Spurious zeros of the Hill determinant do indeed exist [52] for polynomial potentials of the form

$$U_m(x) = \sum_{i=1}^{m} A_i x^{2i}. \tag{72}$$

(2) Spurious and physical solutions can be distinguished by the signs of the associated matrix elements of powers of x [53].

(3) There are certainly no spurious solutions for the quartic anharmonic oscillator ($m=2$) [54] and probably not for any pure-x^{2m} anharmonic oscillator.

(4) The results of Banerjee *et al.* are correct and remain the most extensive set of anharmonic-oscillator eigenvalues in the literature.

Direct Eigenvalue Determination in a Harmonic-Oscillator Basis

The fact that the anharmonic-oscillator energy matrix is banded can simplify diagonalization. Two sets of papers which exploit this possibility are those of Graffi and Grecchi [55] and Hioe *et al.* [8, 56].

Graffi and Grecchi diagonalize in the unperturbed harmonic-oscillator basis, proving monotonic convergence under extensions of the basis by invoking the Rayleigh–Ritz variational principle [30, p. 337]. They give eigenvalues for the states with $N=0$ to 7 of the quartic ($m=2$) anharmonic oscillators with $\lambda=0.2$ and $\lambda=2$ and of the octic ($m=4$) oscillator with $\lambda=0.002$ and $\lambda=0.2$. The accuracy with a basis dimension of 28 is 15 figures for the $m=2$ ground state and 10 for the $m=4$ ground state. Accuracy decreases with increasing m and N.

Hioe *et al.* use the Bargmann representation [57] of the Hamiltonian and wave functions. In this representation they reduce the problem of eigenvalue determination to a search for zeros of the characteristic polynomial.[6] Convergence with increasing basis dimension is studied. Reference [8] lists eigenvalues for $m=2$, $N=0$ to 8, and a range of λ-values from 0.002 to 20,000. A 9-figure accuracy is achieved with a basis of dimension 26. Tables 2B and 2C of Ref. [8] contain a few errors. The eigenvalue for $N=5$ and $\lambda=1$ is given as 14.203 139 4 instead of 14.203 139 1(05); that for $N=7$ and $\lambda=1$ is given as 21.236 436 2 instead of 21.236 435 4(86); the eigenvalue for the state $N=8$ at $\lambda=0.1$ is given as 13.378 969 8 instead of 13.382 478 07; that for $N=8$, $\lambda=1$ is given as 24.994 945 7 instead of 24.994 936 4.

Reference [56] lists eigenvalues for $m=3$ and $m=4$, $N=0$ to 5, and the same range of λ-values as in the paper on the quartic oscillator. Six-figure accuracy is achieved with a basis of dimension 30 for $m=3$, 5-figure accuracy with a basis of dimension 46 for $m=4$.

The basis dimensions and accuracies obtained in these papers for the direct solution of the eigenvalue problem in a harmonic-oscillator basis are consistent with each other and what is found by JWKB–Lanczos methods without rescaling.

Moment Recursion

Richardson and Blankenbecler [15] develop a technique that lies outside the realm of expansions in harmonic-oscillator bases. The essence of their method is to derive and solve recursion relations satisfied by matrix elements $\langle mN|\, x^s \,|mN\rangle$ of powers of x between fixed anharmonic-oscillator eigenstates. Such recursion formulae follow from hypervirial theorems [59, 60]. Richardson and Blankenbecler run the recursion relations for diagonal matrix elements and even s downwards from random values at very large s, much as in the standard numerical method [38, Sect. 5.5] of evaluation of regular Bessel functions. The $s=0$ moment is simply the norm of the wave function; setting this to unity normalizes the entire sequence of moments. The energy then follows from the simple virial theorem (5).

A starting s-value of around 20,000 gives the ground-state energy of the x^4 anharmonic oscillator with $\lambda=1$ to 11 figures, the first excited-state energy to 9 figures, and the second to 7 figures. A starting s-value of 900,000 gives the ground-state energy of the pure-x^4 oscillator to a remarkable 28 figures—by far the most accurate anharmonic-oscillator energy known at the time of publication.

Moment-recursion methods are clearly very powerful. They have the advantage of giving matrix elements of powers of x along with energies. The limited range of applications made to date prevents serious comparison with the JWKB–Lanczos methods used here. It is perhaps noteworthy in this connection that the Lanczos algorithm has intimate connections with moment methods [41, Sect. 2.2].

[6] A similar method for tri-diagonal matrices is discussed in Acton's book [58, pp. 331–335].

Rescaled Inner Projection

The study of Vinette and Čižek [7] uses the rational arithmetic and symbolic manipulation of the programming language MAPLE [31] to evaluate eigenvalues to a precision that is, in principle if not in practice, unlimited. There is of course a price to pay, as there is for the multi-precision calculations mentioned at the end of Section 5; memory requirements increase and computing speeds decrease.

The method used by Vinette and Čižek has much in common with the Lanczos algorithm. It starts with the rescaling transformation (Section 2).[7] The rescaled Hamiltonian of Eq. (21) for ground states—the only cases considered in [7], may be written

$$\mathscr{H}_0^{(m)} = \mathscr{H}_0 + \mathscr{V}^{(m)}, \tag{73}$$

where $\mathscr{H}_0$ is the rescaled harmonic-oscillator Hamiltonian and $\mathscr{V}^{(m)}$ is the residual interaction. (A minor complication enters here; a constant must be added to the residual interaction, to make it positive definite, and subtracted from $\mathscr{H}_{osc}$.) Vinette and Čižek work in the basis introduced in Section 3, spanned by eigenstates of $\mathscr{H}_{osc}$, truncated at dimension $D_0^{(m)}$. A matrix function of the parameter z is then defined in this basis by

$$\mathscr{A}(z) = \mathscr{V} - \mathscr{V}\frac{\Lambda_0}{z - \mathscr{H}_{osc}}\mathscr{V}, \tag{74}$$

where Λ_0 is the projector off the harmonic-oscillator ground state and the label m has been omitted. This matrix function contains an *unperturbed* reduced resolvent and may be evaluated by the methods described in Section 3. An iterative sequence is next defined which brackets the desired rescaled eigenvalue $\mathscr{E} = \mathscr{E}_0^{(m)}$ ever more closely,

$$\mathscr{E}^{k+1} = E_0 + \mathscr{V}(\mathscr{A}(\mathscr{E}^k))^{-1}\mathscr{V}, \tag{75}$$

where E_0 is the energy of the harmonic-oscillator ground-state (minus the constant alluded to above). If $\mathscr{E}^k$ is an upper (lower) bound on the desired eigenvalue, $\mathscr{E}^{k+1}$ is a lower (upper) bound. The eigenvalue is guaranteed to lie between each pair of successive iterates, the region of confinement narrowing as the iterative process proceeds. The main computational task at each iteration is to operate on $\mathscr{V}$ with the inverse of the matrix $\mathscr{A}$; this can be achieved (cf. the discussion following Eq. (54) in Section 5) by solving a system of inhomogeneous linear equations for each column of the matrix.

Vinette and Čižek calculate ground-state energies only, for $m = 2$ to $m = 4$ and for a range of values of λ, including the infinite-coupling limit. The accuracy achieved with basis-dimension $D = 24$ for finite values of λ is 17 figures for $m = 2$, 11 figures for $m = 3$, and 8 for $m = 4$. These are precisely the accuracies obtained with the

[7] Referred to as renormalization in Ref. [7].

JWKB–Lanczos method with the same basis-dimensions. In the infinite-coupling limit the basis dimension is extended to 150. This yields a remarkable level of precision: 62 figures for $m=2$, 34 for $m=3$, and 24 for $m=4$. JWKB–Lanczos reproduces these results precisely; the multi-precision techniques discussed at the end of Section 5 are needed to confirm Vinette and Čižek's results for $m=2$ and $m=3$.

The accuracy achieved for given size of basis seems to be much the same in the rescaled inner-projection and JWKB–Lanczos methods. This suggests that, although seen across the gulf between floating-point and rational-symbolic arithmetic, the two methods have very similar numerical characteristics.

Of the methods discussed in this section, rescaled inner projection seems most promising. It uses rescaling; indeed it was the paper of Vinette and Čižek that first exhibited the full power of the rescaling transformation. There is no obvious barrier to its adaptation to excited states. It would clearly benefit if its variational starting guess were replaced by JWKB. The numerical properties of the method for larger values of m and N and in floating-point arithmetic are of course unknown. The indications are, however, that rescaled inner projection could be developed into a serious competitor to JWKB–Lanczos.

The JWKB Approximation

The first applications of the lowest-order JWKB approximation to the anharmonic oscillator appear in the pioneering paper of Bender and Wu [5]. More extensive numerical applications to the x^4 anharmonic oscillator are to be found in the work of Hioe and Montroll [8, 25]. These lowest-order studies, which already reveal the accuracy of JWKB approximations, use the formalism to be found in standard texts on Quantum Mechanics [24, pp. 268–279]. This formalism, featuring procedures to connect solutions across classical turning points, is difficult to carry to higher orders.

The first study of anharmonic-oscillator spectra to recognize and exploit the power of Dunham's elegant formulation of the JWKB method (Section 4) is that of Krieger *et al.* [35], who compute third-order JWKB energies for the 5 lowest states of the pure-x^{2m} oscillators with $m=2$, 3, 4, $m=6$, and $m=8$. Bender *et al.* [1] compute JWKB energies up to the seventh non-vanishing order for states up to $N=10$ of the pure-x^4 oscillator. To assess the accuracy of high-order JWKB, Bender *et al.* quote exact energies to 21 figures without revealing how they were calculated! All the numerical JWKB results of Hioe and Montroll and of Bender *et al.* have been verified. The only point of disagreement is the value quoted in Table 1 of Bender *et al.* for the energy of the state $N=6$ of the pure-x^4 oscillator. The tabulated value is 26.528 471 883 682 518 191 8; the correct value to 21 figures is 26.528 471 183 682 518 191 8—an obvious error in transcription.

The JWKB calculation for the pure-x^{2m} oscillator is much simpler than for the full anharmonic oscillator. The only published high-order JWKB study of anharmonic-oscillator spectra is that of Kesarwani *et al.* [33, 34]. They compute fifth- and sixth-order JWKB energies for states of the x^4 anharmonic oscillator for about

a dozen values of N from 0 to 20,000, with values of λ at intervals from 0.002 to 1000. Their fifth-order results have been recalculated using the methods described in Section 4; all are confirmed.

Kesarwani and Varshni could not give a clear assessment of the accuracy of the JWKB approximation for very large N because of a lack of sufficiently accurate comparison eigenvalues.

Bacus *et al.* [61] obtain sharp upper and lower bounds for the eigenvalues of the x^4 anharmonic oscillator by techniques closely related to JWKB and to the inner-projection methods alluded to above. They evaluate the 9 lowest eigenvalues of the quartic oscillator to 30 significant figures (confirmed by the JWKB–Lanczos methods described in Section 5). Since they do not rescale, their work is confined to small values of the anharmonicity parameter.

Model- or Reference-Space Methods

Fundamental papers [62–65], published about 40 years ago, deal with the non-Hermitian effective eigenvalue problem obtained by projecting the Schrödinger equation in a large Hilbert space on to a truncated model or reference subspace. These early studies are formal; their aim is the derivation of the effective interaction between nucleons in the nuclear shell model [63] and of the nuclear optical-model potential [64]. Meissner and Steinborn [11] report a numerical application of these model-space techniques, developing an iterative solution of the pertinent non-Hermitian eigenvalue problem. Eigenvalues of the lowest few states of the quartic oscillator are computed both with and without rescaling. The results (confirmed by the JWKB–Lanczos methods described in Section 4) demonstrate the power of the rescaling transformation; with its help 20- to 25-figure precision is obtained for a wide range of values of the anharmonicity parameter.

Perturbation and Strong-Coupling Series

Perturbation expansions for the eigenvalues of anharmonic oscillators are asymptotic rather than convergent for all values of the anharmonicity parameter [17, 66]. Without rescaling, such series yield useful estimates only for very small values of the anharmonicity parameter λ.

Perturbation expansions based on two different partitions of the Hamiltonian into unperturbed and perturbing parts have been considered. That based on the rescaled Hamiltonian of Eq. (10), with expansion parameter κ, has been studied most thoroughly. Variants of the Levin transformation [67] and the Padé–Borel transformation [68] sum the rescaled perturbation series in κ for all eigenvalues of the quartic oscillator to more than 20-figure accuracy for all values of the anharmonicity parameter [21, 69]. The attainable accuracy decreases steadily with increasing m but is still around 8 figures at $m = 6$ [69].

Feranchuk *et al.* [70, 10] and Fernández *et al.* [71] also start with a rescaling transformation of the sort discussed in Section 2. They develop perturbation expansions, of both Rayleigh–Schrödinger and Brillioun–Wigner types. The unperturbed Hamiltonian is defined, not as the rescaled harmonic-oscillator Hamiltonian of

Eq. (10), but as the part of the complete rescaled Hamiltonian diagonal in the rescaled basis. Reasonable accuracy is obtained for low eigenvalues of the quartic oscillator for small values of λ. Improvement is sought [71, 10] by modifying the rescaling parameter from the variational value determined in Section 2. This optimal-scaling procedure is quite successful; accuracies of up to 15 figures are obtained for low-lying states of the quartic oscillator over a wide range of values of λ.

The large-λ strong-coupling expansion (Eq. (17)) has been less-thoroughly explored than have small-λ perturbation expansions. Work has been confined either to formal study of the nature of the expansion [16, 25] or to the difficult problem [26, 9, 27] of computing its coefficients. Promising techniques have been proposed and successfully demonstrated for the first few terms in the series, but the problem has not yet been decisively solved. With the help of accelerative sequence transformations, the strong-coupling expansion can probably yield accurate anharmonic-oscillator eigenvalues over a wide range of λ-values.

8. CONCLUDING COMMENTS

Limitations

A few words are in order about two topics not treated in this paper—wave functions and general polynomial potentials.

Although the eigenvectors associated with the calculated eigenvalues have not been treated explicitly, the necessary information is readily accessible and at minor computational cost. The eigenvectors of interest are given as linear combinations of at most three Lanczos vectors $|\phi_k\rangle$ which in turn are expressed as linear combinations of rescaled harmonic-oscillator basis states. It is then a simple matter to compute the matrix elements $\langle mN|\ \mathcal{O}\ |m'N'\rangle$, diagonal or off-diagonal, of any operator $\mathcal{O}$. The operator must first be expressed in terms of rescaled dynamical variables using the transformation (8). The matrix elements in the rescaled harmonic oscillator basis are then calculated; for powers of x, this can be done using the formulae alluded to in Section 3 or their analogs for odd s. Finally, the appropriate linear combination of harmonic-oscillator matrix elements yields the desired quantity $\langle mN|\ \mathcal{O}\ |m'N'\rangle$.

The general polynomial potential (Eq. (72)) models a physical situation intrinsically richer than that accessible to pure-x^{2m} potentials. Suppose that the coefficient A_m of the highest power of x is positive, so that the polynomial potential has the asymptotic behavior

$$\lim_{|x|\to\infty} U_m(x) = +\infty. \tag{76}$$

This ensures a purely discrete spectrum. The potential can however have internal maxima and minima. The particle can be trapped in the troughs between them. This renders useless the high-order JWKB procedure of Section 4, which assumes

two classical turning points at each energy. Extension to more than two turning points is likely to be prohibitively complicated. It is possible that the variational estimates of Tater and Turbiner [52] can replace JWKB as input to the shifted Lanczos algorithm. However, the difficulties noted by Tater and Turbiner in applying the Hill-determinant method to polynomial potentials with $m = 3$ probably reflect the intrinsic complexity of the underlying physics rather than the limitations of any particular algorithm. No fully automated universal method of the sort that works for pure-x^{2m} anharmonic oscillators is likely to succeed.

Summary

A technique has been devised to calculate, to 33-figure accuracy, all eigenvalues of the x^{2m} anharmonic oscillators with $m = 2$ to 6, for all values of the anharmonicity parameter.

The crucial first step in the procedure is rescaling—introduction of a length scale natural to each state of each of the anharmonic oscillators. This transformation yields an explicitly state-dependent rescaled Hamiltonian; only a single eigenvalue of this Hamiltonian—that corresponding to the state of interest—is physically significant. The introduction of a state-dependent rescaled Hamiltonian is the price paid for the creation of an eigenvalue problem that is finite for all values of the anharmonicity parameter, from zero to the infinite-coupling limit.

The JWKB approximation, carried to five terms ($O(h^{10})$), is then used to estimate the rescaled eigenvalues. This in itself gives 33-figure accuracy for states N higher than a certain critical value that varies linearly from 1500 for $m = 2$ to 3500 for $m = 6$. Even for ground states, the optimum JWKB estimate is accurate to about 10%. Thereafter accuracy increases very rapidly with N.

The remarkable quality of the JWKB approximation suggests that it might with profit be taken as the starting point of a method of "exact" solution of the eigenvalue problem. The shifted Lanczos algorithm, the Lanczos algorithm applied to the resolvent of the Hamiltonian, is well suited to exploit the accurate JWKB starting estimate. With the JWKB energy as the shift parameter, the desired eigenvalue is overwhelmingly larger than all others and the Lanczos algorithm converges with striking rapidity. The 33-figure accuracy is obtained in no more than 3 iterations for any state, in only 2 for $N > 8$, in only 1 for $N > 24$. This very rapid convergence to the single significant eigenvalue of each rescaled Hamiltonian completely defangs the well-known drawbacks of the Lanczos algorithm—slow convergence to non-dominant eigenvalues, loss of orthogonality of the Lanczos vectors. As a means of sharpening a very accurate starting estimate, the shifted Lanczos algorithm is ideal.

Finally, the JWKB–Lanczos method is used to study the systematics of anharmonic-oscillator spectra and to reveal the striking simplifications achieved by the rescaling transformation.

The most significant ways in which this study adds to knowledge of the anharmonic-oscillator eigenvalue problem are the following:

(1) Extension of the rescaling transformation to excited states; detailed study of its physical effects for all states of x^{2m} anharmonic oscillators with $m = 2$ to 6.

(2) Extension of high-order JWKB to anharmonic oscillators with $m = 3$ to 6, for all states and all values of the anharmonicity parameter.

(3) Application of the JWKB approximation to the rescaled rather than to the original Hamiltonian.

(4) Use of the resolvent-based Lanczos algorithm, starting from the JWKB approximation, to evaluate to 33 significant figures the energies of all states of the anharmonic oscillators with $m = 2$ to 6, for all values of the anharmonicity parameter.

(5) Use of the high-precision eigenvalues and their JWKB approximants to fully exhibit for the first time the extraordinary accuracy of the JWKB approximation.

APPENDIX A: SCALING TRANSFORMATIONS

The general form of the x^{2m} anharmonic-oscillator Hamiltonian is

$$H^{(m)}(\omega, \lambda) = \tfrac{1}{2}(p^2 + \omega^2 x^2) + \lambda x^{2m}, \tag{77}$$

where the potential is an arbitrary linear combination (with non-negative coefficients) of x^2 and x^{2m}. The anharmonic-oscillator Hamiltonian and its eigenvalues obey a class of scaling relations, discussed in detail for the quartic oscillator in Ref. [25]. The change of variable

$$x = \omega^{-1/2} y \tag{78}$$

leads directly to the scaling relation

$$H^{(m)}(\omega, \lambda) = \omega H^{(m)}\left(1, \frac{\lambda}{\omega^{m+1}}\right). \tag{79}$$

The change of variable

$$x = \lambda^{-1/2(m+1)} y \tag{80}$$

yields

$$H^{(m)}(\omega, \lambda) = \lambda^{1/(m+1)} H^{(m)}\left(\frac{\omega}{\lambda^{1/(m+1)}}, 1\right). \tag{81}$$

When $\omega = 0$, the general anharmonic-oscillator Hamiltonian (77) reduces to the pure-x^{2m} oscillator of Section 1, Eq. (2),

$$h^{(m)}(\lambda) = H^{(m)}(0, \lambda), \tag{82}$$

and the scaling relation (81) reduces to Eq. (18) in Section 2.

The scaling relations permit the eigenvalues of the general Hamiltonian (77) to be obtained as multiples of those of a reduced Hamiltonian. The reduced Hamiltonian has either an x^2 term (as in the present paper) or an x^{2m} term (as in Ref. [15]) of unit strength. For the pure-x^{2m} oscillator, Eq. (18) gives the eigenvalues for any value of the strength parameter as multiples of the eigenvalues for $\lambda = 1$.

APPENDIX B: CONVENTIONS FOR THE HAMILTONIAN

The literature is almost equally divided between two conventions, differing by a factor 2, for the anharmonic-oscillator Hamiltonian. This apparently trivial matter is a significant hazard in comparing published eigenvalues. The convention used in this paper (Eq. (1)) is that of Bender and Wu [5] and is followed in Refs. [8, 15, 25, 33, 34].

A widely used alternative convention, in which the Hamiltonian is given by

$$H' = p^2 + x^2 + \beta x^{2m} \tag{83}$$

is followed in Refs. [6, 7, 9, 12–14, 16, 21, 46]. The energies, scaling parameters, rescaled coupling strengths, and rescaled energies in this alternative (primed) convention are related to their counterparts in the present paper by

$$E'(\beta) = 2E(\lambda = \beta/2) \tag{84}$$

$$\tau'(\beta) = \tau(\lambda = \beta/2), \qquad \kappa'(\beta) = \kappa(\lambda = \beta/2) \tag{85}$$

$$\mathscr{E}'[\kappa'(\beta)] = 2\mathscr{E}[\kappa(\lambda = \beta/2)]. \tag{86}$$

ACKNOWLEDGMENTS

I thank Brian Serot for many helpful comments and for general encouragement and Ted Barnes for bringing Bailey's multi-precision translation package to my attention. This work was supported by the Department of Energy under Contract DE-FG02-87ER40365.

REFERENCES

1. C. M. Bender, K. Olaussen, and P. Wang, *Phys. Rev. D* **16** (1977), 1740.
2. T. Ericsson and P. S. Jensen, *Math. Comp.* **34** (1980), 1251.
3. B. Nour-Amid, B. N. Parlett, T. Ericsson, and P. S. Jensen, *Math. Comp.* **48** (1987), 663.
4. R. G. Grimes, J. G. Lewis, and H. D. Simon, *SIAM J. Matrix Anal. Appl.* **15** (1994), 2.
5. C. M. Bender and T. T. Wu, *Phys. Rev.* **184** (1969), 1231.
6. J. P. Killingbeck, *J. Phys. A* **18** (1985), 245.
7. J. L. Vinette and J. Čižek, *J. Math. Phys.* **32** (1991), 3392.
8. F. T. Hioe and E. W. Montroll, *J. Math. Phys.* **16** (1975), 1945.
9. R. Guardiola, M. A. Solís, and J. Ros, *Il Nuovo Cim. B* **107** (1992), 713.

10. I. D. Feranchuk, L. I. Komarov, I. V. Nichipor, and A. P. Ulyanenkov, *Ann. Phys.* (*N.Y.*) **238** (1995), 370.
11. H. Meissner and E. O. Steinborn, *Int J. Quantum Chem.* **61** (1997), 777.
12. S. N. Biswas, K. Datta, R. P. Saxena, P. K. Srivastava, and V. S. Varma, *J. Math. Phys.* **14** (1973), 1190.
13. K. Banerjee, S. P. Bhatnagar, V. Choudry, and S. S. Kanwal, *Proc. R. Soc. London A* **360** (1978), 575.
14. J. P. Killingbeck, "Microcomputer Quantum Mechanics," Hilger, Bristol, 1983.
15. J. L. Richardson and R. Blankenbecler, *Phys. Rev. D* **19** (1979), 496.
16. B. Simon, *Ann. Phys.* (*N.Y.*) **58** (1970), 76.
17. C. M. Bender and T. T. Wu, *Phys. Rev. Lett.* **27** (1971), 461.
18. E. Brézin, J.-C. Le Guillou, and J. Zinn-Justin, *Phys. Rev. D* **15** (1977), 1544.
19. E. Brézin, J.-C. Le Guillou, and J. Zinn-Justin, *Phys. Rev. D* **15** (1977), 1558.
20. S. Graffi, V. Grecchi, and B. Simon, *Phys. Lett. B* **32** (1970), 631.
21. E. J. Weniger, J. Čižek, and F. Vinette, *J. Math. Phys.* **34** (1993), 571.
22. I. N. Sneddon, "Special Functions of Mathematical Physics and Chemistry," Oliver & Boyd, Edinburgh, 1956.
23. H. Goldstein, "Classical Mechanics," 2nd ed., Addison–Wesley, Reading, MA, 1980.
24. L. I. Schiff, "Quantum Mechanics," 3rd ed., McGraw–Hill, New York, 1968.
25. F. T. Hioe, D. MacMillen, and E. W. Montroll, *Phys. Rep. C* **43** (1978), 306.
26. A. V. Turbiner and A. G. Ushveridze, *J. Math. Phys.* **29** (1988), 2053.
27. F. M. Fernández and R. Guardiola, *J. Phys. A* **26** (1993), 7169.
28. J. H. Wilkinson, "The Algebraic Eigenvalue Problem," Oxford Univ. Press, London, 1965.
29. L. Morales and A. Flores-Riveros, *J. Math. Phys.* **30** (1989), 393.
30. K. Gottfried, "Quantum Mechanics," Addison–Wesley, Reading, MA, 1989.
31. B. W. Char, K. O. Geddes, G. H. Gonnet, M. B. Monagan, and S. M. Watt, "MAPLE Reference Manual," 5th ed., Watcom, Waterloo, Ontario, 1988.
32. H. Jeffreys, *Proc. London Math. Soc.* **23** (1923), 428.
33. R. N. Kesarwani and Y. P. Varshni, *J. Math. Phys.* **22** (1981), 1983.
34. R. N. Kesarwani and Y. P. Varshni, *J. Math. Phys.* **23** (1982), 803.
35. J. B. Krieger, M. L. Lewis, and C. Rosenzweig, *J. Chem. Phys.* **47** (1967), 2942.
36. J. L. Dunham, *Phys. Rev.* **41** (1932), 713.
37. M. H. Macfarlane, to be submitted for publication.
38. W. H. Press, S. A. Teukolsky, W. T. Vetterling, and B. P. Flannery, "Numerical Recipes; the Art of Scientific Computing," 2nd ed., Cambridge Univ. Press, Cambridge, UK, 1992.
39. B. N. Parlett, *J. Num. Lin. Alg. Appl.* **1** (1992), 243.
40. R. Haydock, *in* "Computational Methods in Classical and Quantum Physics" (M. B. Hooper, Ed.), Advance Publications, London, 1976.
41. R. R. Whitehead, A. Watt, B. J. Cole, and I. Morrison, *in* "Advances in Nuclear Physics" (M. Baranger and E. Vogt, Eds.), Vol. 9, Plenum, New York, 1977.
42. C. C. Paige, *J. Inst. Math. Appl.* **10** (1972), 373.
43. J. J. Dongarra, J. R. Bunch, C. B. Moler, and G. W. Stewart, "LINPACK Users' Guide," Soc. for Industr. & Appl. Math., Philadelphia, 1978.
44. C. C. Paige, *J. Inst. Math. Appl.* **18** (1976), 341.
45. D. H. Bailey, *ACM Trans. Math. Software* **19** (1993), 288.
46. K. Banerjee, *Proc. R. Soc. London A* **364** (1978), 265.
47. N. Bazley and D. Fox, *Phys. Rev.* **124** (1961), 483.
48. D. P. Datta and S. Mukherjee, *Phys. Rev. A* **13** (1980), 3161.
49. S. Flessas, *J. Phys. A* **15** (1982), L1.
50. S. Flessas and G. S. Agnostatos, *J. Phys. A* **15** (1982), L537.
51. R. N. Chouduri, *Phys. Rev. D* **31** (1985), 2687.
52. M. Tater and A. V. Turbiner, *J. Phys. A* **26** (1993), 697.

53. J. Killingbeck, *J. Phys. A* **19** (1986), 2903.
54. J. Killingbeck, *J. Phys. A* **18** (1985), L1025.
55. S. Graffi and V. Grecchi, *Phys. Rev. D* **8** (1973), 3847.
56. F. T. Hioe, D. MacMillen, and E. W. Montroll, *J. Math. Phys.* **17** (1976), 1320.
57. V. Bargmann, *Rev. Mod. Phys.* **34** (1962), 829.
58. F. S. Acton, "Numerical Methods That Work," Harper & Row, New York, 1970.
59. J. Killingbeck, *Phys. Lett. A* **65** (1978), 87.
60. K. Banerjee, *Phys. Lett. A* **63** (1977), 223.
61. B. Bacus, Y. Meurice, and A. Seumadi, *J. Phys. A* **28** (1995), L381.
62. C. Bloch, *Nucl. Phys.* **6** (1958), 329.
63. C. Bloch and J. Horowitz, *Nucl. Phys.* **8** (1958), 91.
64. H. Feshbach, *Ann. Phys.* (*N.Y.*) **5** (1958), 357.
65. H. Feshbach, *Ann. Phys.* (*N.Y.*) **19** (1962), 287.
66. F. M. Fernández, A. M. Mesón, and E. A. Castro, *Phys. Lett. A* **104** (1984), 401.
67. E. J. Weniger, *Comp. Phys. Rep.* **10** (1989), 189.
68. S. Graffi, V. Grecchi, and B. Simon, *Phys. Lett. B* **32** (1970), 631.
69. M. H. Macfarlane, to be submitted for publication.
70. I. D. Feranchuk and L. I. Komarov, *Phys. Lett. A* **88** (1982), 211.
71. F. M. Fernández, A. M. Mesón, and E. A. Castro, *Phys. Lett. A* **112** (1985), 107.